Synthesis, stability and antifungal properties of glutathione stabilized Ag nanoclusters

Vikram Singh Bhati

A dissertation submitted for the partial fulfilment of BS-MS dual degree

Indian Institute of Science Education and Research Mohali

April 2017

Dedicated to Parikshit

Certificate of Examination

This is to certify that dissertation titled by **"Synthesis, stability and antifungal properties glutathione stabilized Ag nanoclusters"** submitted by **Mr. Vikram Singh Bhati** (Reg. No. MS12068) for the partial fulfilment of BS-MS dual degree programme of the institute has been examined by the thesis committee duly appointed by the Institute. The committee find the work done by candidate satisfactory and recommends that the report be accepted.

Dr. Arijit K. De Dr. Sabyasachi Rakshit Dr. Ujjal K. Gautam

(Supervisor)

Dated

April, 2017

Declaration

The work presented in this dissertation has been carried out by me under the guidance of Dr. Ujjal K. Gautam at the Indian Institute of Science Education and Research Mohali.

This work has not been submitted in part or in full for a degree, a diploma, or a fellowship to any other university or institute. Whenever contribution of others are involved, every effort is made to indicate this clearly, with due acknowledgement of collaborative research and discussion. This thesis is bonafied record of original work done by me and all sources listed within have been detailed in bibliography.

Vikram Singh Bhati

(Candidate)

Dated: April 21, 2017

In my capacity as the supervisor of the candidate's project work, I certify that the above statements by the candidate are true to the best of my knowledge

Dr. Ujjal K. Gautam

(Supervisor)

Acknowledgement

It is my privilege to express my sincere gratitude to my supervisor **Dr. Ujjal K. Gautam** for his guidance and invaluable discussion throughout this work. Additionally I am very thankful to him for exposing me to this interesting field of research. In his lab, I have been meticulously treated; I have got fruitful time to inculcate my knowledge. In our group collegiums, I have had appreciable scientific conversation with all group people, and he allowed me to enhance my calibre in this field.

I am pleased to acknowledge Prof. N. Sathyamurthy and Prof. K.S. Viswanathan for their motivation and inspiration. I would like to thank my committee members Dr. Arijit K. De and Dr. Sabyasachi Rakshit. I am thankful to Dr. Samrat Ghosh, Dr. A. R. Choudhury and Prof. Anand K. Bachhawat for their timely help and providing lab facility to my research. I am happy to acknowledge IISER-Mohali for providing me facilities like IR, HRMS, UV- Vis Spectrometer, XRD etc. I am thankful to DST, New Delhi for providing INSPIRE fellowship.

I am extremely thankful to my all labmates Moumita, Sanjit, Lipi, Neeru, Kautsav, Dr. Arabindo in particular Dr. P. Essaki karthik for his valuable suggestions, advice and support during my thesis work. I am thankful to Shambhu Yadav for helping me with anti-fungal activity test experiments.

I am very exuberant to mention all my friends for making me always happy in IISER-Mohali. During hard times, I have received many positive comments from those people, which strengthen my inner minds. I have learnt many lessons from all of my friends; personally, I felt it made me to an erudite status in this society. All my alacrity and perseverance, I have got from my friends. They are Nitesh, Shrinit, Varsha, Akshya, Bhupendra, Prem, Maruthi, Mukesh, Ashish, Abhijit, BK, Rudra, Omprakash.. I have felt these are all treasures; I have got from my friend without paying anymore effort.

Also Last but not least I would like to thank my parents and brother Bharat Singh Bhati for always standing behind me with love and support.

List of figures

List of tables

Abbreviations

1. NCs	Nanoclusters
2. Ag-ML	Ag cluster mother liquor
3. PAGE	Poly acryl amide gel electrophoresis
4. BSA	Boven serium albuin
5. RT	Room temperature
6. SEM	Scanning electron microscope
7. GSH	Glutathione
8. $Agcl_{WR}$	Wine red Ag clusters
9. $Agcl_{W}$	White Ag clusters
10. $Agcl_{R}$	Regenerated Ag clusters
11. $Agcl_{RT}$	Room temperature synthesis Ag clusters
12. MALDI	Matrix-assisted laser desorption Ionization

Contents

Abstract

Ag nanoclusters consist of a few to few hundreds of atoms having sizes that are comparable to the Fermi wavelength of electrons and exhibit fascinating molecule-like properties such as discrete electronic transitions and strong fluorescence. However, stabilising these clusters is extremely difficult due to their reactive nature leading to oxidation and also inherent nature of agglomeration. We have synthesized glutathione (GSH) capped Ag clusters (<2 nm) which forms a wine red colour dispersion in water. We have examined their stability and observed that over time, colour of this solution fades down due to surface oxidation of these clusters. We have further found that the Ag clusters shows antifngal activity towards pathogenic fungus *Candida albician*, while it doesn't show any such activity towards nonpathogenic fungus *Saccharomyces cerevisiae.* Since it is known that the antifungal activity scales to reactive oxygen species (ROS) concentration, we propose that the generation of ROS is preferentially triggered by the pathogenic fungus in this case.

1. Introduction

1.1 What are nanoclusters ?

Nanoclusters are particles which have size of less than 2 nm and have been attracting attention for their unique role in bridging the "missing link" between atomic and nano particle behaviour[1]. These nanoclusters are unique in that they can be represented with definite formulas and they represent organic-inorganic hybrid system. Plasmon absorption disappears completely for nanoclusters. Besides, size of nanoclusters is comparable or less than the fermi wavelength of electrons which induces nanoclusters to exhibit molecule-like behaviour[2]. As a result of discrete electronic states, cluster shows size dependent fluorescence[3]. These phenomena are fundamentally very interesting and also of practical importance which makes nanoclusters distinct from the nanoparticles. Semiconductor quantum dots, which were discovered before nanoclusters, also act as a fluorescence label for many biological diagnosis and treatment. However presence of heavy metals such as Cd, Pb and Se in quantum dots drastically affect the environment as well as human cell during diagnostics, hence heavy metal free fluorescence probe is an important to develop[4,5]. Because of non-invasive property of the noble metal clusters, these are promising for application in these fields. Moreover, nanoclusters sizes fit with emission energies via the simple relation, $E_{fermi} / N^{1/3}$, predicted by the spherical jellium model. Emission energy decreases with increasing number of atoms[7]. Though nanoclusters have demonstrated excellent performance towards anti-fungal activity, the synthesis of appropriate nano-clusters is still challenge.

1.2 Approaches and challenges in nanoclusters synthesis

Most of the nanoclusters synthesis is followed a bottom–up procedure because the nanocluster synthesis through top-down method is tedious. In the bottom up procedure, arresting the growth of the particles post nucleation for controlling the number of atom in cluster is an important step. Fortunately many organic compounds serve as a capping agent to control the nucleation and produce the appropriate metal clusters. In another approach, the growth of clusters can be controlled by template assisted synthesis. Some important nanocluster synthesis methodologies are briefly described below.

The template- assisted synthesis bio molecules: Herein proteins such as BSA (bovine serum albumin) or DNA or dendrimers (e.g. poly(amidoamine)(PAMAM)) or polymer (e.g.

poly(meth acrylic acid) (PMAA) are used as templates to control the nucleation process and particle growth.[8,9] The most widely employed capping agents are usually bio-chemicals such as glutathione, insulin, homocystein; organo-phoshporous – oligonucleotide; organo thiol-mercaptobenzoic acid (MBA), mercapto propionic acid (MPA) etc. As discussed later, in our Ag cluster synthesis, less toxic glutathione is used as a capping agent and sodium borohydride is acting as a reducing agent.[10,11].

1.3 Factors affecting cluster nature

The metal cluster properties are highly oriented with particle size and capping agents[12]. Stevenson *et al.* reported the size dependant catalytic activity of clusters towards *p*-nitrophenol reduction, in which case, the smaller clusters (size less than *ca*. 10 nm) didsn't show any activity towards nitro phenol reduction[13]. Jeybharathi et al. observed change in the (ORR) oxygen reduction reaction mechanism on gold surface from 2 electron to 4 electron transfer while changing nanoparticles to cluster[14]. The size dependant UV-Vis absorption spectra was also reported by David *et al*[15], which indicated that the electronic absorption changes with respect to the size of the clusters. Such observation inferred that the electronic levels changes with respect to cluster size (figure 1).

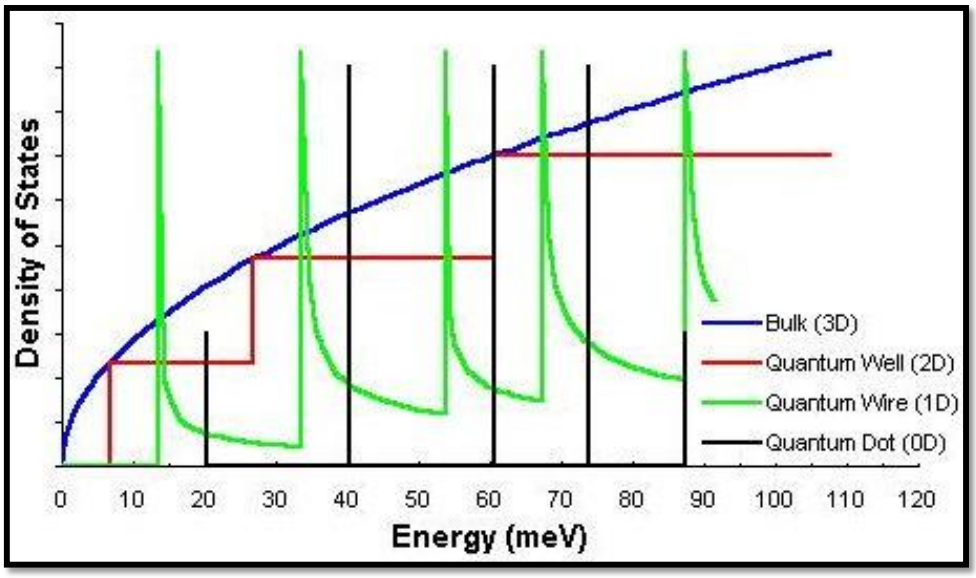

Figure.1. *Distribution of all the possible quantum states per unit volume per unit energy that electrons in the metal can take* [6]

Similar to the cluster size, capping agent plays major role for determining cluster properties .The capping agent assisted cluster properties have been investigated for several reaction mechanism and molecular architecture, for e.g., thiol and amine protected clusters decoration on gold surface[16]. The decoration of these clusters was done with the help of capping agent. Same way the clusters surface charge can be tuned by using different types of capping agents such as, positive negative and neutral gold clusters have been reported.

When we tune the ratio of substrate - capping agent, the cluster size can be changed. For example, mixtures of different-sized GSH-protected Au NCs could be synthesized by using GSH-to-Au ratio of 3 : 1 and $NaBH_4$ ($NaBH_4$-to-Au ratio = 10 : 1) as the reducing agent. *Negishi et. al.* carried out a similar synthesis (GSH-to-Au ratio = 4 : 1, and $NaBH_4$-to-Au ratio = 10 : 1) and successfully identified nine types of Au NCs species with discrete sizes [from $Au_{10}(SG)_{10}$ to $Au_{39}(SG)_{24}$] by using PAGE. *Kumar et. al.* observed 16 types of Ag clusters by varying GSH-Ag concentration (4: 1) and using $NaBH_4$ ($NaBH_4$-to-Ag ratio = 10 : 1) as the reducing agent[17,18] .

Enormous amount of efforts have been availed for improving the mono-dispersed clusters or enhance the color purity of photoluminescence nanoclusters, such as manipulating the metal-thiolate complex intermediates, thiol etching, slowing down the reduction kinetics[19]. Recent report shows that the poly-disperse non fluorescent thiol protected silver nanoclusters can be converted into mono-dispersed highly fluorescent nanoclusters by using phase transfer method.

The above mentioned method, initially as synthesised poly-dispersed metal NCs transfer into organic phase like toluene or hexane by using phase transfer agent e.g., CTAB. The electrostatic interaction between negatively charged carboxylic groups of capping agent and positively charged cation of hydrophobic salt (CTAB) as shown in figure (2) assisted this process. The low kinetics of thiol etching can help to generate the formation of mono-dispersed Ag cluster. In this organic phase, thiol etching is much slower as compared to in aqueous medium and we can also synthesis mono-dispersed nanoclusters[20].

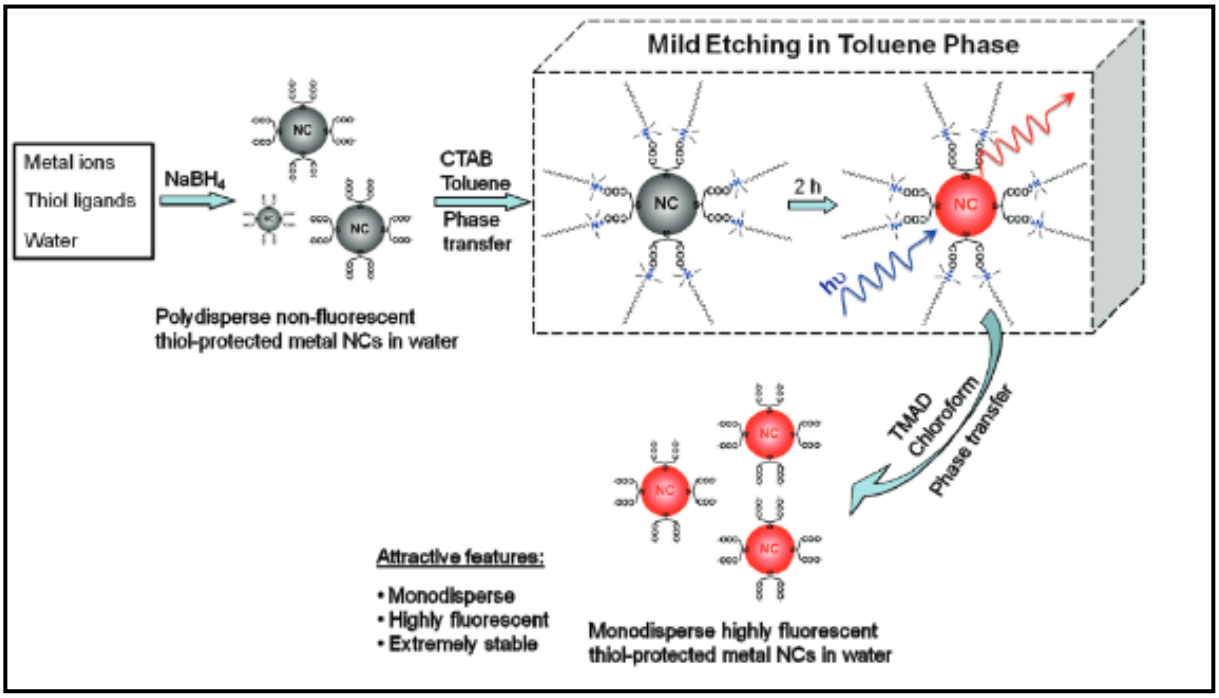

Figure 2. *Schematic illustration of the process to generate highly fluorescent metal NCs by a phase transfer cycle (aqueous – organic(incubation) - aqueous)*[13].

The synthesis of mono-dispersed peptide protected metal nanoclusters could also be achieved by slowing down the reduction kinetics. *Yao et. al.* developed a method to reduce the reduction kinetics to get mono-dispersed metal nanoclusters, that is limiting the concentration of the soluble Au (i) – SG complex intermediate and adding an organic phase containing relatively less reactive reducing agent. The concentration of the soluble Au (i)- SG complexes was regulated by controlling the pH sensitive aggregation dissociation equilibrium of the Au(i) – SG complexes. Net charges on the GSH ligand was determined by the pH, so pH affects the solubility of the intermediate into water. Instead of strong reducing agents like $NaBH_4$, relatively weak reducing agent Borane tert-butylamine (TBAB) in toluene can slow the reduction rate because of diffusion of base from organic phase to aqueous phase[21].

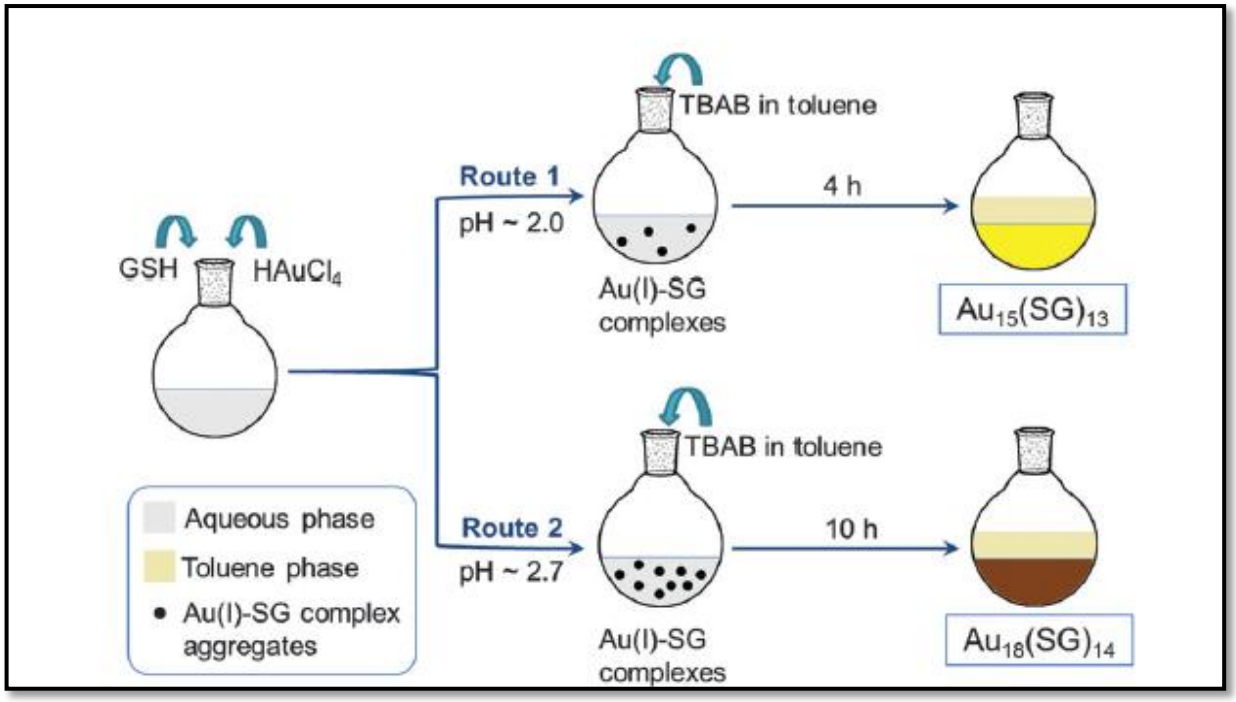

Figure 3.*Schematic illustration of two-phase synthesis of mono-dispersed gold nanoclusters*[14].

.

High thermal assisted synthesis of noble metal cluster is creating problem because at high temperature, very difficult to control the cluster nucleation kinetics. It prevents as to increase the temperature to avoid agglomeration. Thermal assisted cluster agglomeration controlled us to use the high temperature for evaporating water molecule; hence we prefer to use high vacuum evaporation[22].

1.4 Applications of nanoclusters

1.4.1. In biology

Nanoclusters with core size smaller than 2 nm have unique physical and chemical properties like intense luminescence, discrete electronic structure; defined molecular structure etc. For using anti-microbial application the cluster size should be less than 5 nm because most of the living organism cell size less than ca. 5 nm. At this size, the cluster particles can easily be introduced within cell machinery without too much interference. Understanding of biological processes on the nanoscale level is a strong driving force behind development of nanotechnology. Wherefore nanoclusters are having enormous application in biomedical field such as bioimaging, biosensing, antimicrobial agents, detection of protein, probing of DNA structure and cancer therapy. When we use any material for biological system, biggest problem comes is biocompatibility[23,24]. To fulfil this purpose enormous research has been

done on Ag and Au nanoclusters. These noble metal clusters are very much biocompatible with human body.

1.4.2. Sensor

Nanoclusters are also having application in heavy metal sensing. Heavier and toxic metals can be detected by using metal nanoclusters in the way of either decreasing (fluorescence quenching) or increasing fluorescence intensity. As we know, nitrite widely exists in ground and surface water system and it is a hazardous pollutant as well. It can produce a precursor for the production of highly carcinogenic N- nitrosamines upon interaction with protein which causes disease like esophageal cancer and infant methemoglobinemia. Those diseases are incubated from nitrite accumulation in liver. *Yuon et.al.* shows that hyperbranched polyethylenimine protected Ag nanoclusters (hPEI-Ag NCs) shows decrease in fluorescence intensity in the presence of nitrite, in this way it can selectively and detect nitrite at low concentration level[25].

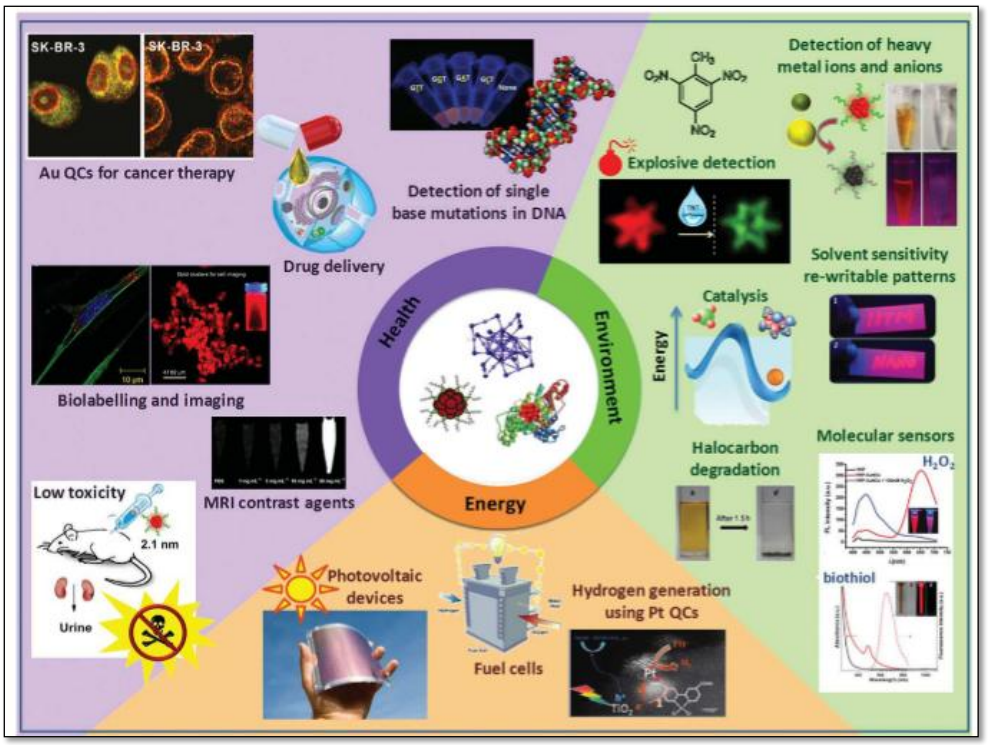

Figure 4. *Figure showing applications of nanoclusters in various field.*

1.4.3. Catalysis

The metal cluster is having different surface properties than metal nanoparticles; hence the catalytic activity of this metal cluster changes drastically. The changed surface and electronic property of this cluster is useful for energy conversion reactions[26]. The gold assisted CO_2 reduction is also reported by Rongchavo Jin. He observed that the high activity towards electrochemical reduction of CO_2 on Au25 cluster surface and CO formation from CO_2 with low over potential was observed, which is in comparable with bulk gold, 200-300 mV over potential smaller than bulk.

1.4.4. Overview of our work

In recent years, severe fungal infections have significantly contributed to the increasing mortality of patients who have weak immune system. So there is great need to synthesise antifungal medicine to overcome this problem.

We have worked on nanoclusters antifungal property and interesting feature showed by nanoclusters is that it is preferentially showing antifungal activity towards pathogenic fungus *candida ablician* and remain inactive towards non-pathogenic fungus *Saccharomyces cerevisiae. Saccharomyces cerevisiae* is a species of yeast and has been used in winemaking, baking and brewing since very long time. It comes under the non pathogenic fungus category i.e. it does not affect human body.

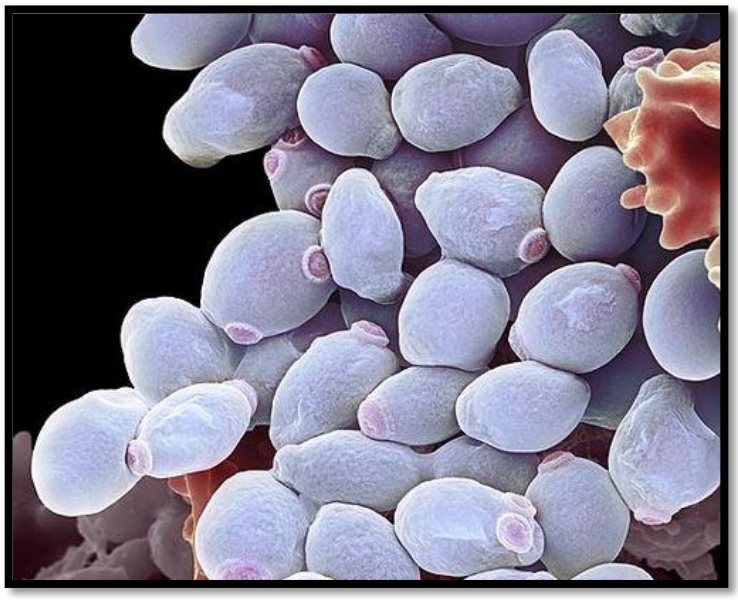

Figure 5. *Photomicrograph of the fungus Candida albicans*

Candida albician is a fungus, which comes under the pathogenic fungus category and grows both as yeast and filamentous cells, causing the candidiasis in humans. There are 20 species of Candida yeasts that can cause infection in humans; the most common is *Candida albicians*. It is responsible for 50-90% of all cases of candidiasis in humans. *Candida albicians* is a common member of human gut flora and it is usually commensal organism but can become pathogenic in individuals with weak immune system whose overgrowth can result in candidiase. It frequently occurs on mucous memberanes in the mouth or vagina, but may affect another regions of body. Candidiasis that develops in the mouth or throat is called "thrush" or orpharyngeal candidiasis. Candidiasis in the vagina is commonly referred to as a "yeast infection". When candida species enter the blood stream and spread throughout the body it's called invasive candidiasis[27-30].

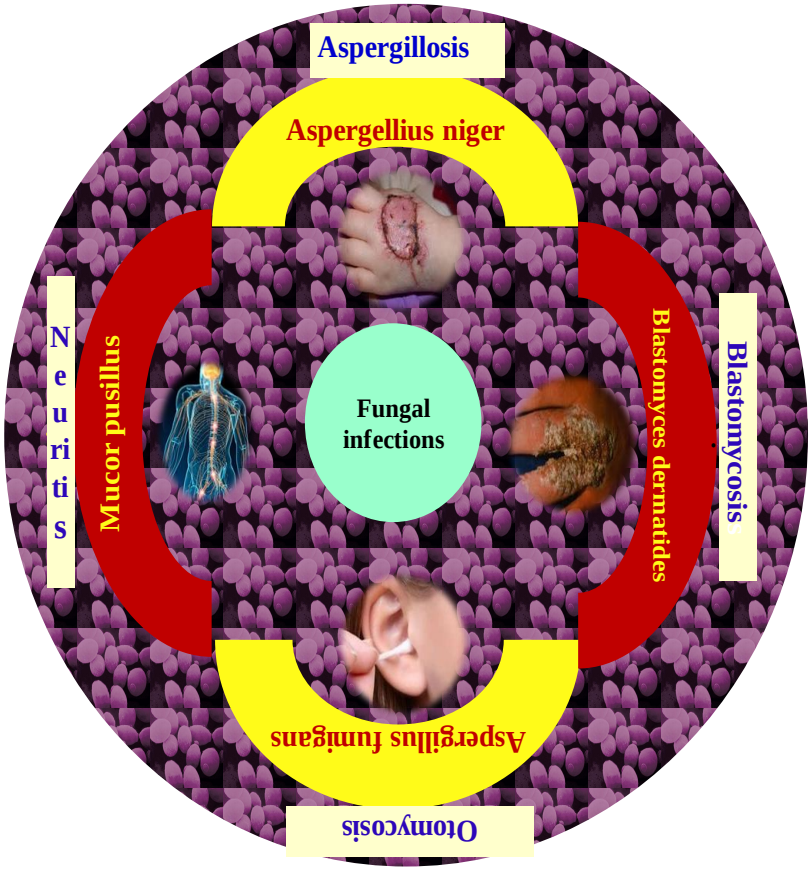

Figure 6. *Graphical illustration of different types of fungal disease.*

2. Experimental Section

2.1 Chemicals

The following reagents were purchased from Sigma Aldrich: Sodium Borohydride ($NaBH_4$), Silver Nitrate ($AgNO_3$), Glutathione (GSH), Chloroauric acid ($HAuCl_4$), Sodium Hydroxide (NaOH), Nickel Nitrate ($NiNO_3$), Tetramethylenediamine (TEMED), Sodiumdodecyl Sulphate (SDS), Acrylamide, Bisacrylamide, Ammonium Persulphate. Methanol (Spectrochem), Yeast, Distilled water. All the chemicals were commercially available and used without further purification.

2.2 Synthesis

We have adopted following procedure for synthesising different types of silver clusters, and the named following based on experimental conditions and appearance:

1) Wine red colour Ag clusters ($Agcl_{WR}$)
2) White Ag clusters ($Agcl_{W}$)
3) Regenerated Ag clusters ($Agcl_{R}$)
4) Synthesis of Ag nano clusters at RT ($Agcl_{RT}$)

2.2.1 Synthesis of $Agcl_{WR}$

42.4 mg (0.25 mmol) of $AgNO_3$ was dissolved in 50 ml of Distilled water and 307 mg of GSH (1 mmol) was added to above $AgNO_3$ solution. This reaction mixture was kept at ice cold condition for 30 minutes which turned into white cloudy suspension, indicating complex formation between Ag and GSH, which infers the formation of low soluble Ag-thiol complex. This complex is an important intermediate for synthesising thiol protected noble metal cluster synthesis.

92.4 mg (2.5 mmol) of reducing agent $NaBH_4$ was dissolved in 12.5 ml distilled water and this reaction mixture was kept at ice cold condition. To avoid the hydride loss from $NaBH_4$, the solution was used immediately and added drop wise to $AgNO_3$ solution at 11000 RPM stirring rate to reduce silver ion (Ag^+). White cloudy solution turned slowly yellow and after some time it became dark brown (wine red) in colour. The reaction mixture was maintained at stirring condition for an hour. This reaction mixture was taken for synthesis of all types of cluster. It was considered as mother solution, named as Ag-ML.

This reaction mixture (Ag-ML) has been concentrated up to 8-10 ml by using high vacuum at RT because high temperature may affect the cluster stability. The Ag cluster was precipitated using 25ml methanol using anti-solvent method; which was washed by ultrasonic dispersion followed by continuous centrifugation. At last the precipitate was dried under vacuum to get Ag clusters in powder form.

2.2.2 Synthesis of white Ag clusters

To synthesis the white colour Ag clusters, Ag-ML solution was preserved at room temperature for 24 hours .The Ag-ML solution colour disappears from dark brown to colourless. Such colour change can be attributed to the change in the cluster composition. Now this colourless solution was concentrated to 8-10 ml using high vacuum at RT. 25 ml of methanol was added into this solution, resulting in immediate white colour precipitation. The precipitate was separated and washed by ultrasonic dispersion and centrifugation for three times with the help of methanol. At last precipitate was dried under vacuum to get Ag clusters in powder form.

2.2.3 Synthesis of regenerated Ag clusters

For preparing the regenerated silver cluster from Ag-ML solution, the Ag-ML was kept at RT for 24 hours. Similar to previous case, the colour of the solution turns from brown to colourless. Again 92.4mg of $NaBH_4$ was dissolved in 12.5 ml distilled water and added to the reaction mixture drop wise at 1100 RPM stirring rate to control the cluster nucleation, the solution became again dark brown. Now this solution was concentrated to 8-10 ml using high vacuum and Ag clusters was precipitated by adding 25 ml methanol. The precipitate was separated and washed by ultrasonic dispersion and centrifugation for three times with the help of methanol. At last precipitate was dried under vacuum to get Ag clusters in powder form.

2.2.4 Synthesis of Ag nano clusters at RT

To study the cluster stability and temperature effect, we have synthesised the Ag cluster at room temperature by using above procedure. Instead of using ice-cold condition, in this procedure all the processes were done at RT and it has been named as Room temperature Ag clusture (RT-AgCl). Moreover, the water evaporation was performed at 60˚ C with help of rotary evaporator.

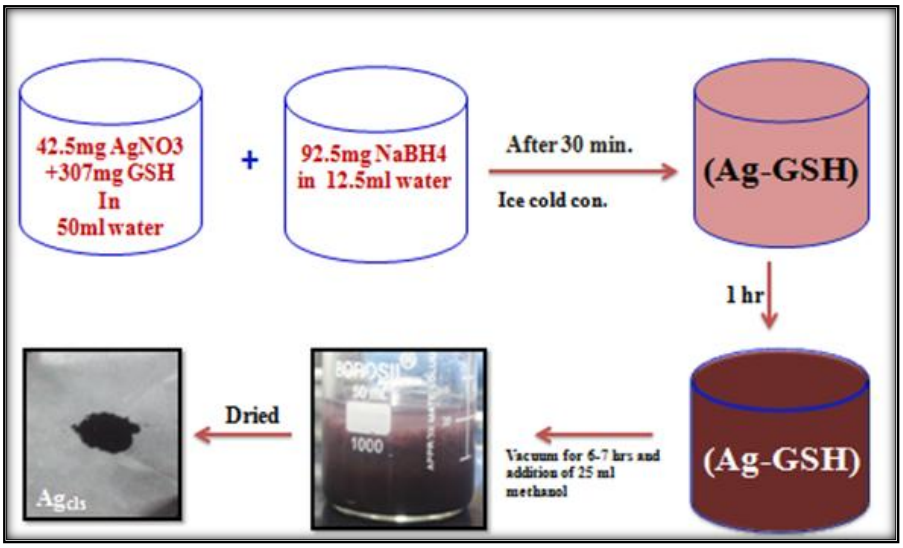

Figure 7. *Schematic illustration of Ag clusters synthesis*

2.3 Material characterization

i) Powder X-Ray Diffraction

ii) Scanning Electron Microscopy

iii) Energy Dispersive X-ray Analysis

iv) Fourier Transform Infrared Spectroscopy

v) UV-Visible Spectroscopy

vi) Poly Acrylamide Gel Electrophoresis

vii) Photoluminescence Spectroscopy

viii) Matrix Assisted Laser Desorption Ionization- Time Of Flight Analyzer

ix). Thermogravimetric Analysis

x) Anti-fungal activity of Ag clusters on pathogenic and non-pathogenic fungi by measuring by Optical density (OD) of the cells using Biophotometer (growth curve assay)

xi) Growth assay by dilution spotting.

2.3.1 Powder X-ray diffraction (PXRD)

The Ag metal cluster lattice parameter and metallic nature was analysed by XRD analysis. Different types of Ag clusters (as mentioned above) were analysed, using PXRD machine from Rigaku Ultima IV company fully automatic high resolution X- ray diffractometer system equipped with a 3kW sealed tube Cu Kα X-ray radiation (generator power settings : 40kV and 40mA) and DTex Ultra detector using parallel beam geometry. The samples were placed on a Si sample holder and analysed over an angle range from 20˚ to 80˚ at a scan rate of 5˚/min. The XRD penetration depth was *ca.* 1 µm, hence, for avoiding background Si signal, the sample thickness was maintained more than 1µm.

2.3.2 Scanning Electron Microscope (SEM)

The morphology of the samples was analysed using Field Emission Scanning Electron Microscopy (FE-SEM) JEOL-JSM-7600F. Sample was drop-casted on Si wafer and solvent was evaporated and after that SEM images were recorded. The FE-SEM was operated with an accelerator voltage of 20-30 KV and a chamber pressure of 10^{-5} torr.

2.3.3 Energy Dispersive X-ray Analysis (EDXA)

To confirm the attachment of Glutathione to Ag clusters, elemental analysis was performed. EDXA spectra showed the presence of both Ag and S. The EDXA area mapping was done for an hour.

2.3.4 Fourier Transform Infrared Spectroscopy

Fourier Transform Infrared (FTIR) spectral analysis was performed to identify the chemical functionality of synthesised Ag-cluster species. All the FTIR analysis was performed using Perkin Elmer FT-IR 2-Spectrometer, and the spectrum was recorded using KBr pellet. The anhydrous KBr pellet was made with *ca.* 2mg of our substrate (Ag-cluster species) for FTIR analysis. To attain the homogeneous substrate distribution on KBr pellet, anhydrous KBr salt and substrate was grinded using a mortar and pestle, with the help of vacuum gauge, pellets were made.

2.3.5 UV-Visible Spectroscopy

UV spectra for all types of Ag clusters were recorded using UV 3000+ LABINDIA spectrophotometer. The optical spectra were measured by quartz cuvette of 1cm path length at RT. All the spectrum was recorded at same scan rate (5nm/s) and wavelength window of 800 to 200 nm. To maintain the appreciable UV-Vis absorbance for studying electronic nature of cluster, aqueous solution of Ag clusters were prepared in the concentration of 2.5mg/5ml. The stability of the Ag-ML was investigated at different conditions (Nitrogen atmosphere – ice cold condition, Nitrogen atmosphere – RT, Ice cold condition in open air atmosphere) using UV-Vis spectrum. (Detailed discussion in Results and discussion section 3.1)

2.3.6. Poly Acrylamide Gel Electrophoresis (PAGE)

The inspiration has come from biological protein molecule (Macro-molecule analysis) analysis by electrophoresis method. The same methodology was adopted to analyse the number of different types of Ag clusters and their charges. In this analysis, gel with 30% concentration of acrylamide monomer and 4% bis-acrylamide cross-linker for resolving gel was used to analyse, in particular number of different size of Ag clusters. The gel dimensions were 8 cm X 10 cm. The gel was run at constant voltage 150V. 50µl of sample was loaded in each well.

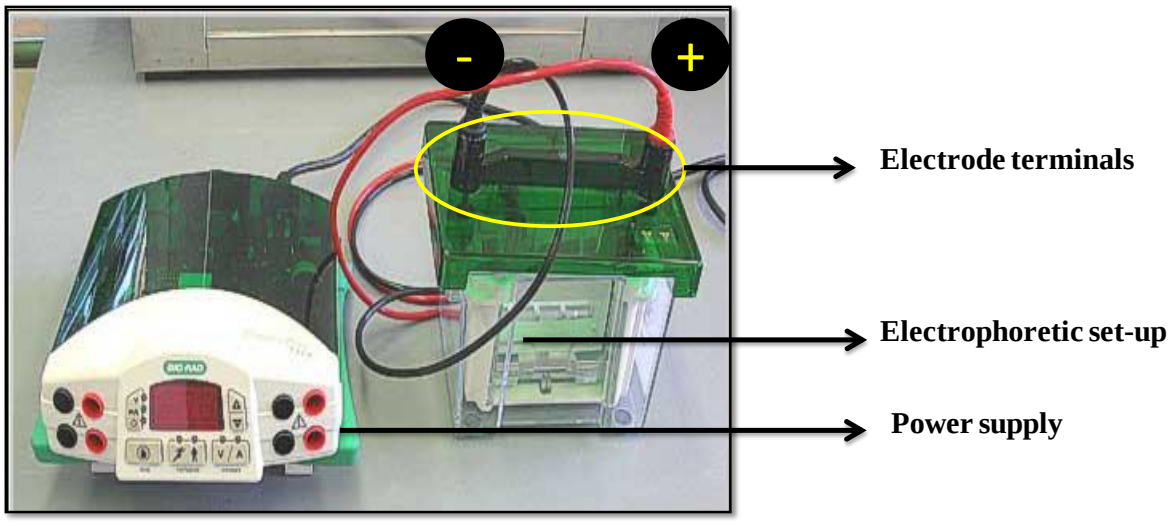

Figure 8. *Photograph of Electrophoresis Instrument for PAGE analysis.*

2.3.7. Photoluminescence Spectroscopy

Fluorescence spectra for silver clusters were recorded with help of RF-6000 SHIMADZU spectrofluorometer. For reducing signal to noise ratio (S/N), the spectra was recorded with the slit-width of 5nm X5nm, and the scan rate was maintained at 5 nm/s. For comparison, Ag clusters do not show any fluorescence activity.

2.3.8. Matrix-assisted laser desorption Ionization-Time of flight (MALDI-TOF)

Mass spectra of $Agcl_{WR}$ clusters, $Agcl_{W}$ clusters and $Agcl_{R}$ clusters were recorded using MALDI.

Figure 9. *Photograph of MALDI-TOF instrument*

Matrix Assisted Laser Desorption Ionization – Time Of Flight (MALDI-TOF) mass spectroscopy is based on the principle of bombardment of samples with a laser to undergo sample ionization. Initially, the sample is with a highly absorbing matrix compound for the most consistent and reliable results (for example, α-cyano-4-hydroxycinnamic acid, Sinapinic acid etc.) and a low concentration of sample was used for better efficiency of the matrix. The matrix transforms the laser energy into excitation energy for the sample, which leads to sputtering of analyte and matrix ions from the surface of the mixture. In this way, energy transfer is efficient and also the analyte molecules are spared excessive direct energy that may otherwise cause decomposition. Most commercially available MALDI mass spectrometers now have a pulsed nitrogen laser of 29 wavelength 337 nm. The time-of-flight analyzer separates ions according to their mass (m)-to-charge(z) (m/z) ratios by measuring the time it takes for ions to travel through a field-free region known as the flight, or drift,

tube. The heavier ions are slower than the lighter ones. The m/z scale of the mass spectrometer is calibrated with a known sample that can either be analyzed independently (external calibration) or pre-mixed with the sample and matrix (internal calibration). MALDI is also a "soft" ionization method and so results predominantly in the generation of singly charged molecular-related ions regardless of the molecular mass, hence the spectra are relatively easy to interpret and fragmentation does not usually occur.

2.3.9 Thermogravimetric Analysis

Thermogravimetric analysis (TGA,Shimadzu DTG-60H) was done to find out content of Ag and glutathione in glutathione capped Ag clusters. 3.5-4.0 gm of sample was heated treated in alumina crucible for 30˚ to 800˚ at a constant heating rate of 5˚C/min under N_2 atmosphere (flow rate 30 ml/min) TGA was done.

2.3.10. Anti-fungal activity of Ag clusters on pathogenic and non-pathogenic fungi by measuring Optical density (OD) of the cells using Biophotometer (growth curve assay)

For growth curve assay, the wild type Candida albican strain (AB2240) was grown overnight in rich medium YPD (yeast peptone and dextrose) and reinoculated in fresh medium to an OD600 of 0.1 in YPD medium containing 50µM concentration of $Agcl_{WR}$ (1) , $Agcl_{W}$ (2), $Agcl_{R}$(3), $Agcl_{RT}$ (4). Optical density was measured using POLAR star Omega in every one and half hour till 18 to 20 hours or till growth was saturated and graphs were plotted using Origin.

2.3.11.Growth assay by dilution spotting

For routine culture, cells from stocks stored at −80 °C were propagated by streaking onto Yeast-peptone-dextrose (YPD) agar plates (1% yeast extract, 2% peptone, 2 % dextrose, and 2.2 % agar), and the wild type Candida albican strain (AB2240) was grown overnight in rich medium YPD at 30°C and reinoculated in fresh medium to an OD600 of 0.1 and grown for 4 hours. The exponential phase cells were harvested washed with water and resuspended in water to an OD600 of 0.2. These were serially diluted to 1:10, 1:100 and 1:1000. 10 µl of these cell re-suspended were spotted on YPD medium containing 50µM concentration of $Agcl_{WR}$ (1), $Agcl_{W}$ (2), $Agcl_{R}$ (3), and $Agcl_{RT}$ (4). The plates were incubated at 30ºC for 2 to 7 days and photographs were taken using BIO-RAD Gel Doc.

3 Results and discussions

3.1 UV-Vis absorption spectra

3.1.1 UV-Vis absorption spectra of solid Ag clusters

Wine red solid Ag clusters show absorbance peak at 498 nm as shown in figure 10. Generally, Ag clusters show absorption maximum at approximately 470 nm. The UV-Vis absorption spectrum of our Ag clusters also exhibit a shoulder peak at 487 nm, matching various other literature reports[31] Electrons in the cluster gets excited when exposed to electromagnetic energy leading to the UV-Vis absorption peak. In addition, another tiny peak appeared at 364 nm, which is not reported so far. The origin of the new peak is not clear at this moment. It is possible that charge interaction between sulphur lone pair and Ag surface responsible for this transition.

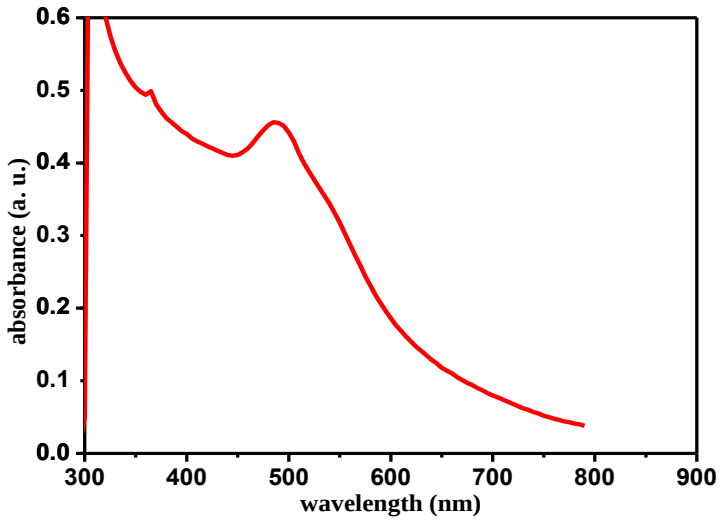

Figure 10. *UV-Vis absorption spectrum of solid Ag clusters with concentration 3 mg /1.5 ml.*

3.1.2 UV-Vis absorption spectra of Ag clusters in mother liquor

It was reported that the clusters made by this method are highly unstable if left in the mother liquor. The powder collected from the mother liquor after a few hours formation is white in color. A similar color transformation occurs with the dry clusters as well when dispersed in water, though at a slower pace. On the other hand, it is sometimes essential keep them in solution for at least a few hours or else one needs to find a strategy to regenerate

them. The stability of the Ag clusters dispersed in mother liquor was monitored using UV-Vis absorption spectroscopy. As seen in Figure 11, the intensity of the absorption peak decreased drastically until ~100 hours. At the same time, the solid Ag clusters stability was also monitored after dispersing them in water. They have shown much higher stability and the decrease in intensity of the absorption peak even after a month is much less than the clusters dispersed in mother liquod for 4 days, as elaborated in section 3.1.4.

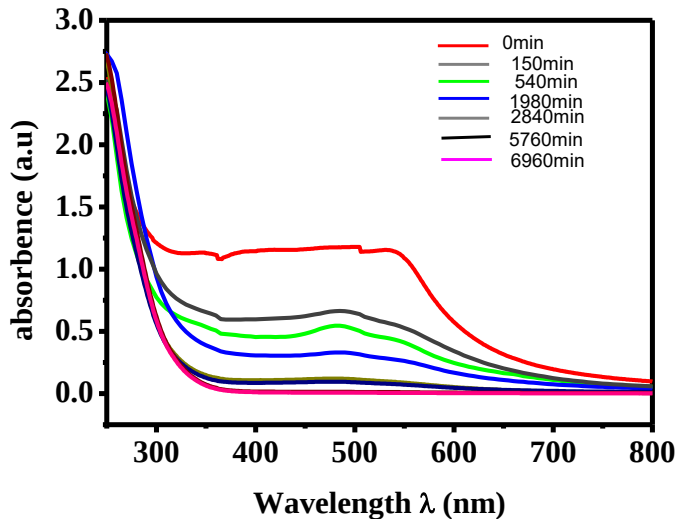

Figure 11. *Absorption spectra of Ag clusters left in mother liquor showing decrease in intensity with time.*

3.1.3 UV-Vis absorption spectra of Ag clusters kept at different environment

We have also done experiments to find out the effect of atmospheric oxygen on the disappearance in the colour of mother liquor solution of Ag clusters. For this we kept mother liquor in nitrogen atmosphere, in an open environment (at ice cold and RT). We observed that initially UV absorbance peak intensity was different for all the above solutions but after 96 hours it becomes same for all the sample.

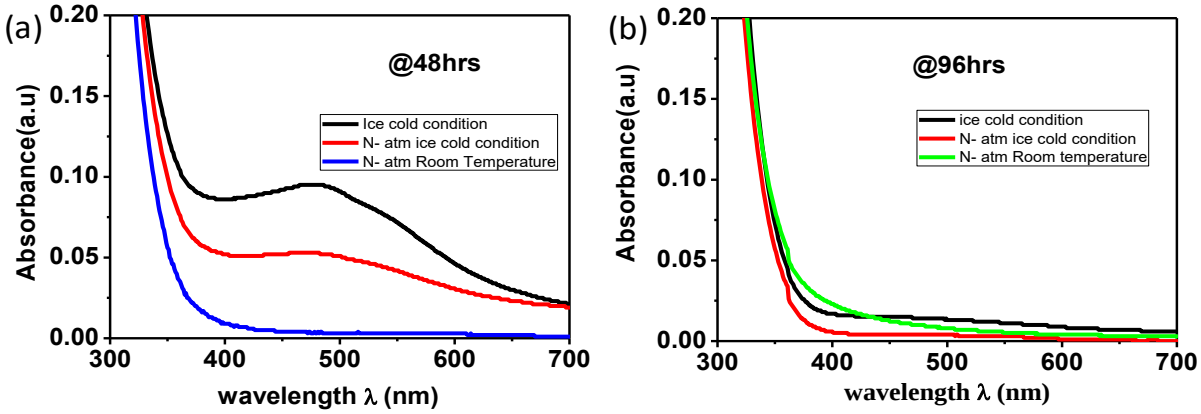

Figure 12. *UV-Vis absorption spectra of Ag clusters kept under different atmospheric conditions. (A) UV-Vis absorption spectra taken after 48 hours. (B) UV-Vis absorption spectra taken after 96 hours.*

3.1.4 UV-Vis absorption spectra of wine red solid Ag clusters recorded at different time

The wine red mother liquor solution is not stable with time as shown in the above results. The intensity of UV-Vis absorption peak for wine red Ag clusters becomes zero with time. But if we disperse solid Ag clusters in water, then the intensity of UV-Vis absorption @ 490 nm peak does not go to zero even after 37 days.

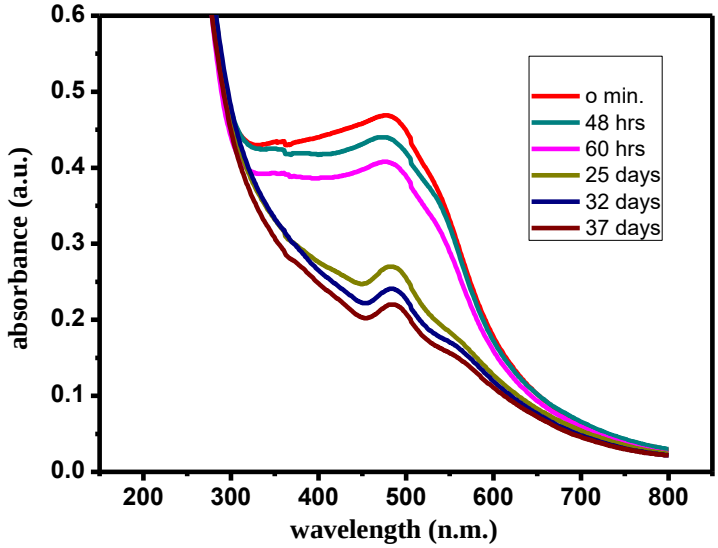

Figure 13. *UV-Vis absorption spectra of wine red powder Ag clusters recorded at different time.*

3.1.5 Regeneration of the colour and UV-Vis absorbance peak

As known, the colour of mother liquor solution changes from wine red to colorless in 116 hrs and its UV-Vis intensity also decreases with time.

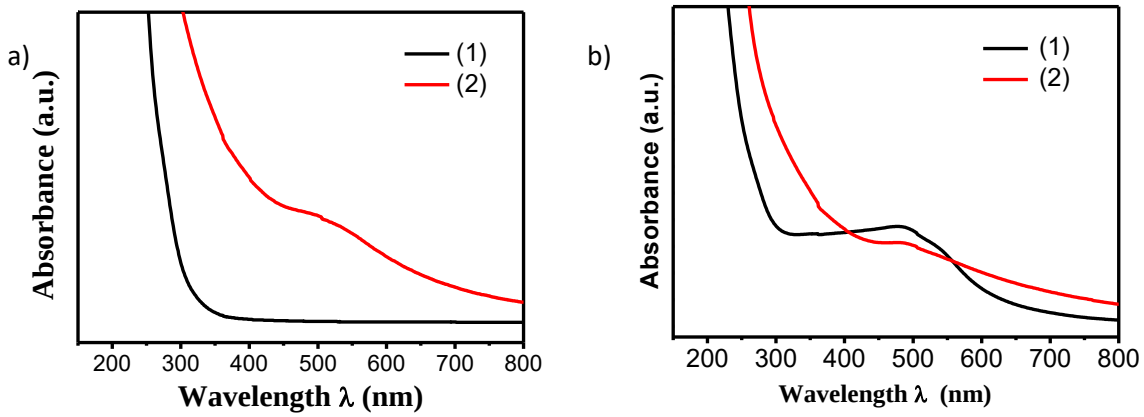

Figure 14. *(a) UV-Vis absorption spectrum of white mother liquor (shown by black line) and that of white mother liquor after addition of $NaBH_4$ (shown by red line) (b) UV-Vis absorption spectrum of white solid Ag clusters dispersed in water with (2 mg/5 ml, shown by red line) and UV-Vis absorption spectrum of solid wine red Ag clusters (2 mg/5 ml, shown by black line).*

However, if we add $NaBH_4$ to the colorless solution, then wine red color reappears and we also found that the UV-Vis absorption peak corresponding to wine red solution appear again. Similarly, when we added $NaBH_4$ to white solid clusters, we found that the peak as well as color reappears.

3.2 Fourier Transform Infra Red spectroscopic studies

IR spectrum of glutathione shows peak at 2500 cm $^{-1}$ which corresponds to the stretching frequency of S-H bond whereas in the case of wine red and white Ag clusters, there is no peak corresponding to S-H bond being found. This shows that there is covalent interaction between sulphur atom of glutathione molecule and Ag[22].

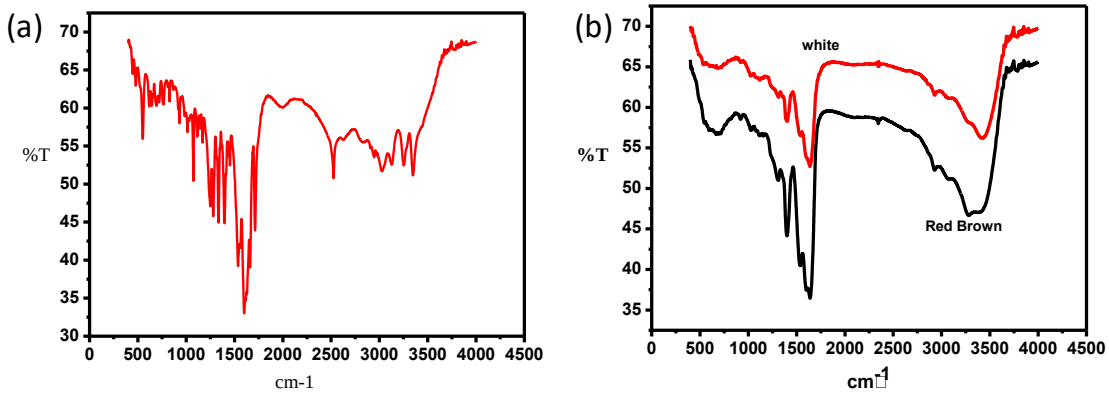

Figure 15. *(a). IR spectrum of glutathione showing peak at 2500 cm^{-1} (b) IR spectra of white and wine red Ag clusters (showing disappearance of S-H peak).*

3.3 Energy Dispersive X-ray Spectroscopy studies

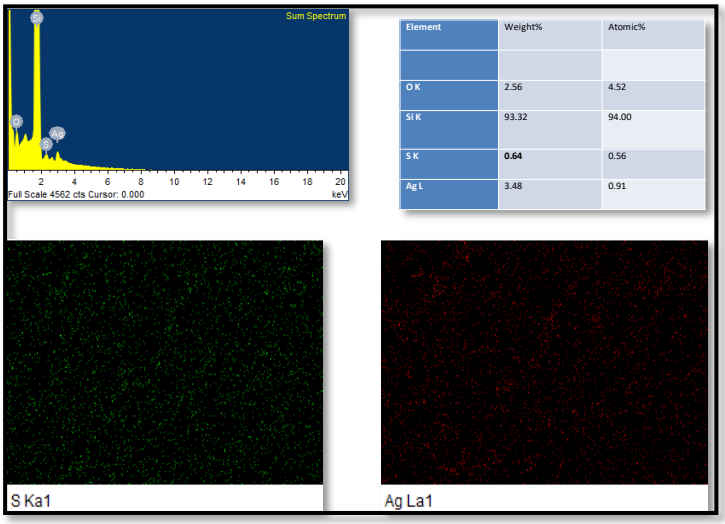

Figure 16. *EDS spectrum and elemental mapping confirming presence of both Ag and S.*

EDS was performed on a random assembly of Ag clusters distributed on Si substrate, showing that our clusters are composed of both Ag and sulphur. The percentage of Ag is found to be 71 while sulphur is approximately 29%.

3.4 Scanning Electron Microscopy studies

The morphology of Ag clusters has been investigated through SEM and is presented in Figure 17. The image doesn't show any individual cluster particles, instead the network arrangement of cluster particles was observed. This network arrangement could implicate that the formed glutathione protected silver cluster molecules are interacting among themselves and developing a dendrimers like structure.

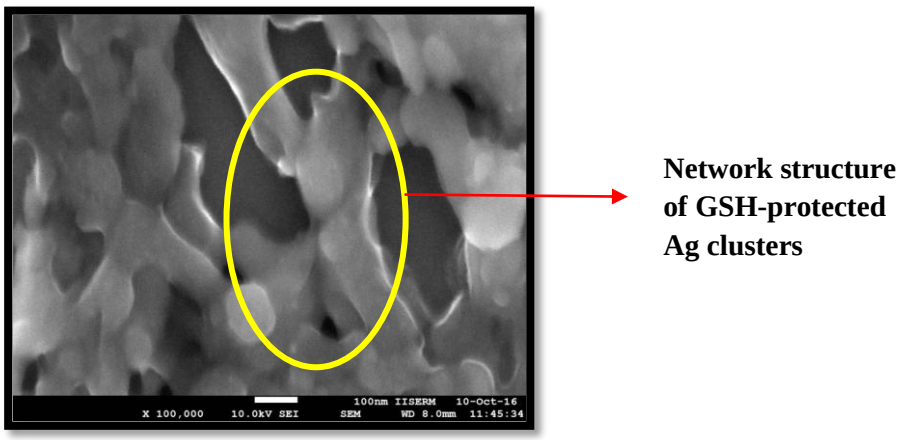

Figure 17. *SEM image of glutathione protected Ag nanoclusters.*

The formation of this type of dendrimers structure can easily be explained by the self assembly of nanoparticles[32]**.** This self assembly of nanocluster particles has recently showed many applications in the field of molecular electronics. Here, we have found our Ag cluster self–assembly through SEM analysis, the science behind this self assembly of Ag clusters are further investigated in our laboratory.

3.5 Poly Acrylamide Gel Electrophoresis (PAGE) study

Different bands in PAGE were seen which clearly indicated the presence of different sized Ag clusters in powder. As shown in figure 18, the bands are not fully resolved due to the small size of gel being used for the study (8 cm x 10 cm). We also found that the colour of various bands are not same which futher validates the presence of chemically different species in the mixture[33].

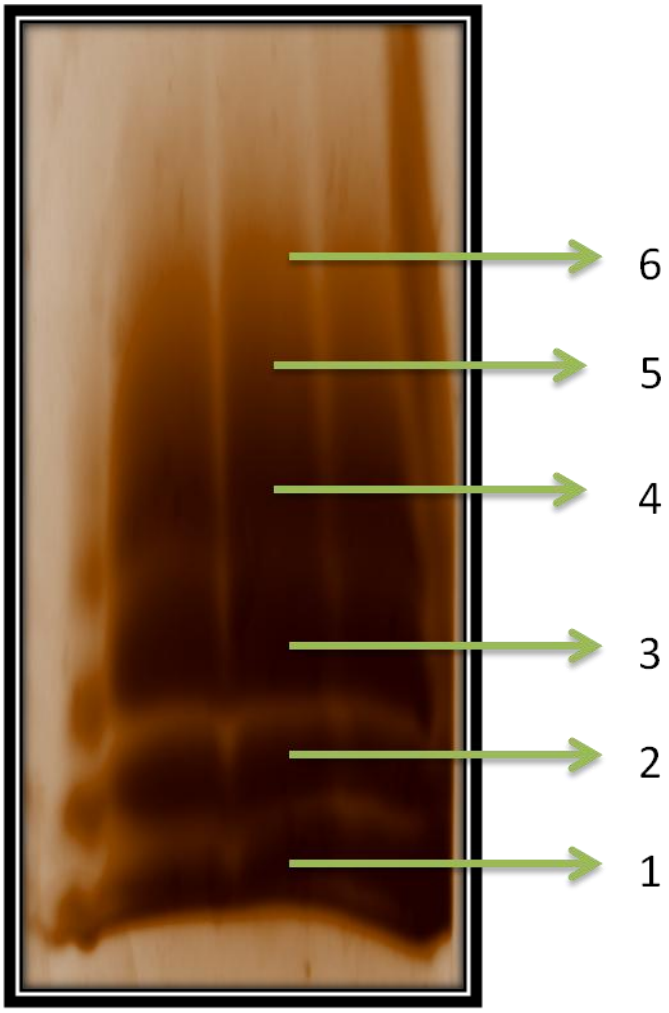

Figure 18. *PAGE image of Ag clusters.*

3.6 Matrix Assisted Laser Desorption (MALDI) study

The MALDI spectra of glutathione, wine red, white and regenerated Ag clusters are presented in the figure 19a, b, c and d respectively. The formation of Ag clusters was confirmed through MALDI spectrum for each type of cluster synthesis. The glutathione peak was cancelled by prior analysis of glutathione MALDI-TOF pattern. It has given clear idea about the numbers of silver atoms present in every silver cluster particles. The number of peaks and apparent calculated silver atoms are tabulated in table 1, 2, 3, 4. Moreover, the exact charge of as formed silver cluster was not known, all the calculations are made with the assumption that silver is having +1 charge. The as-obtained MALDI-TOF patterns were matched with previous literature[34].

Table (1). List of glutathione mass peaks obtained from figure 19a

S.No.	Peak position	Comment
1.	179.12	Fragment
2.	233.12	Fragment
3.	308	GSH
4.	330	Na-GSH

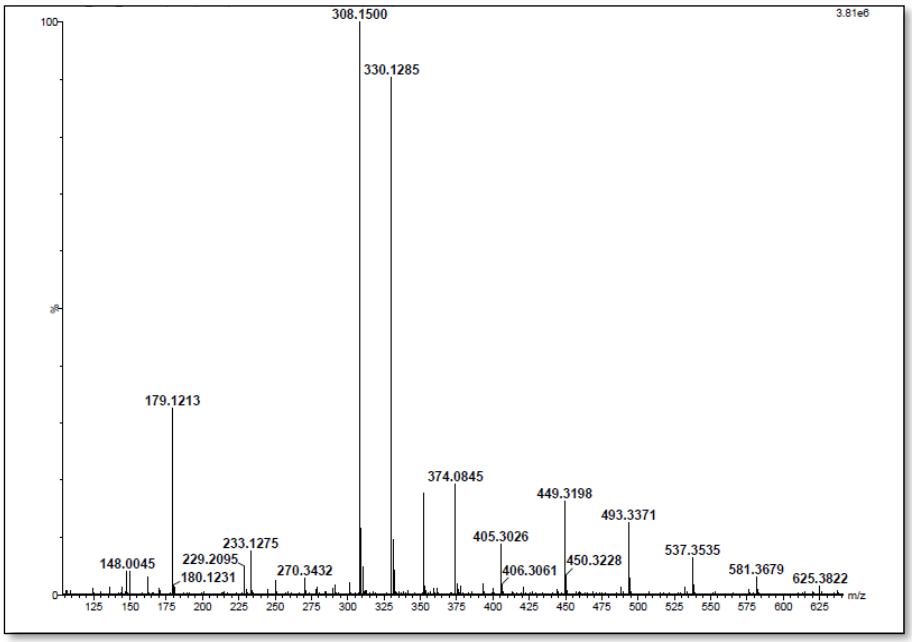

***Figure 19 (a)**. MALDI spectrum of glutathione.*

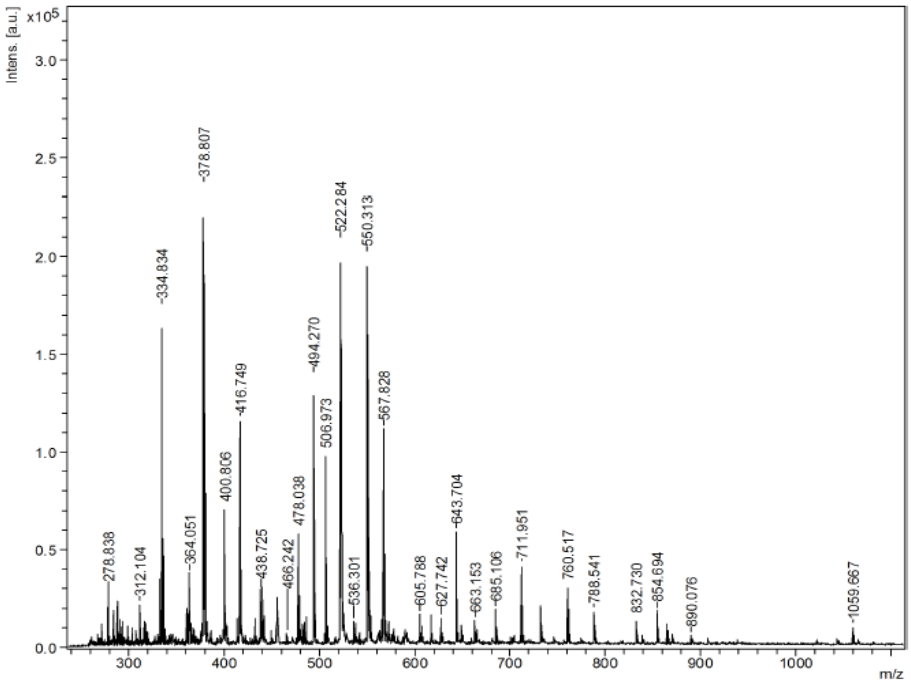

Figure 19(b). *MALDI-TOF spectrum of wine red Ag clusters.*

Table (2). List of peaks obtained from the wine red sample seen in figure 19b.

S. No.	Position(m/z)	Formula	Comments
1.	278.83	**GSH**	**GSH fragmentation**
2.	334.83	**Na-H_4.GSH**	**Sodium adduct**
3.	364.05	**Na-$(H_2O)_2$-GSH**	**Hydrated form of GSH**
4.	378.80	**Na_3-GSH**	**Sodium adduct**
5.	400.08	**Na_4-GSH**	**Sodium adduct**
6.	416.74	**Ag-GSH**	**Single adduct**
7.	494.27	**HCOONa-O_2-Na-GSH**	**Oxygen format adduct of GSH**
8.	506.97	**(Ag-GSH)Na_4**	**Sodium adduct of Ag-GSH**
9.	522.28	**Ag_2SG**	**Glutathione adduct with 2 Ag**
10.	550.03	**[Ag_2GSH].$(BH_3)_2$**	**Sodium adduct of Ag_2 cluster**
11.	567.82	**(Na-Ag_2GSH)-H_2O**	**Hydrated Na adduct of Ag_2 cluster**
12.	643.70	**HCOONa-Ag_2-$(OH)_3$ – GSH**	**Na format adduct of Ag cluster**
13.	711.95	**[Ag_3-BO_3-$(H_2O)_2$]-GSH**	**BO_3 adduct of Ag_3 cluster**
14.	740	**Ag4-GSH**	**GSH protected Ag_4 cluster**

15.	760.51	**$[Ag_3(HCOONa)_2]$-GSH**	**Na format adduct of Ag_3 cluster**
16.	1059.66	**Ag_7-$(H)_2$GSH**	**GSH protected Ag_7 cluster**

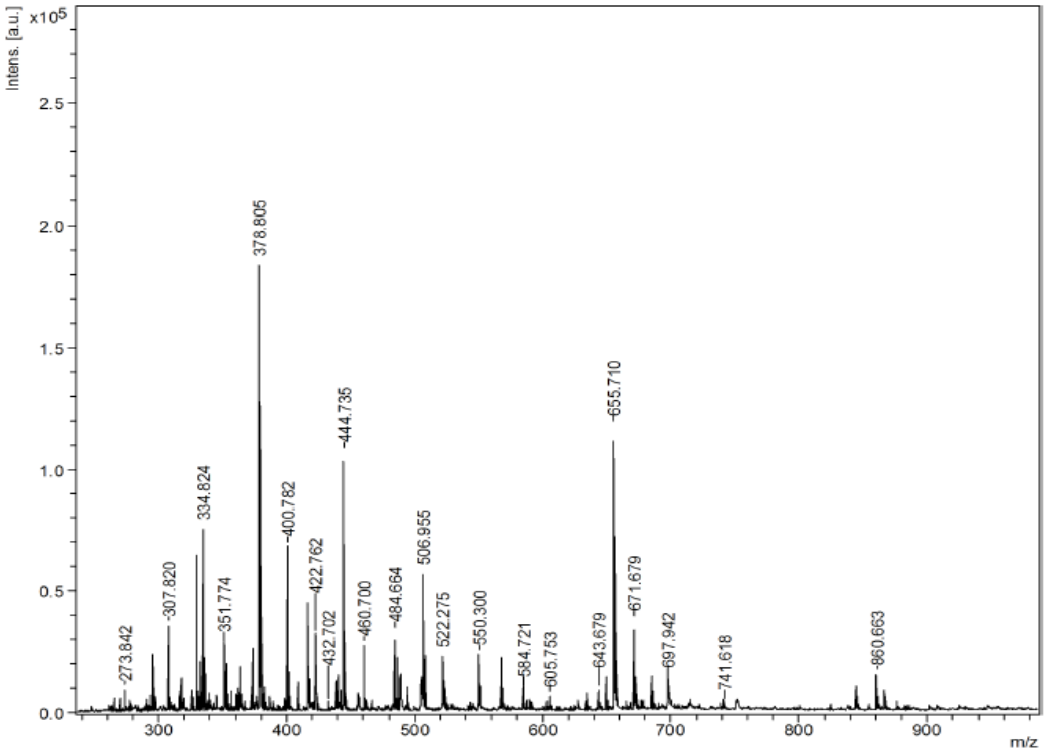

Figure 19(c). *MALDI spectrum of white Ag clusters.*

Table 2. List of peaks obtained from the white sample seen in figure 19c.

S. No.	Peak position	Formula	Comments
1	307.82		**Glutathione peak**
2.	334.82	**Na-H_4.GSH**	**Sodium adduct**
3.	378.80	**Na_3-GSH**	**Sodium adduct**
4.	400.78	**Na_4-GSH**	**Sodium adduct**
5.	418.12	**(Na_4- GSH) H_2O**	**Hydrated form of Sodium adduct of GSH**

6.	422.76	**Na_5 - GSH**	**Sodium adduct of GSH**
7.	444.73	**Na_6 - GSH**	**Sodium adduct of GSH**
8.	460.70	**Ag- Na_2- GSH**	**Sodium adduct of Ag GSH**
9.	484.66	**Ag- Na_3- GSH**	**Sodium adduct of Ag GSH**
10.	506.95	**(Ag-GSH)Na_4**	**Sodium adduct of Ag-GSH**
11.	522.27	**Ag_2SG**	**Glutathione adduct with 2 Ag**
12.	550.30	**[Ag_2GSH].(BH_3)$_2$**	**Sodium adduct of Ag_2 cluster**
13.	567.30	**(Na-Ag_2GSH)-H_2O**	**Hydrated sodium adduct of Ag_2 cluster**
14.	643.679	**HCOONa-Ag_2-$(OH)_3$ - GSH**	**Sodium format adduct of Ag cluster**
15.	655.71	**(Ag_3- GSH)Na**	**Ag_3 cluster**
16.	671.67	**[(Ag_3-GSH)Na]. H_2O**	**Hydrated form of Ag_3 clusters**
17.	697.94	**(Ag_3- SG-HCOONa)**	**Ag_3 cluster**
18.	860.66	**[Ag- GS-O]$_2$**	**Ag cluster**

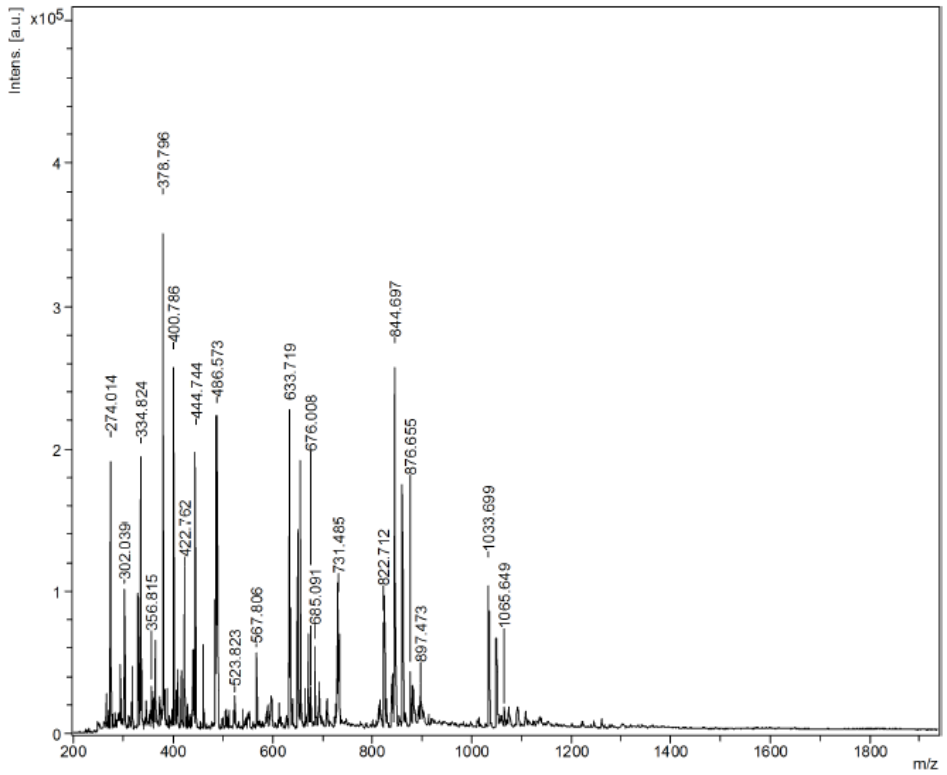

Figure 19 (d). *MALDI spectrum of regenerated Ag clusters.*

Table 4. Peaks of regenerated of Ag clusters obtained from figure 19d.

S. No.	Peak position	Formula	Comments
1.	274.0	-	**Fragment GSH**
2	334.82	**Na-H_4.GSH**	**Sodium adduct**
3.	378.80	**Na_3-GSH**	**Sodium adduct**
4.	400.78	**Na_4-GSH**	**Sodium adduct**
5.	422.76	**Na_5 - GSH**	**Sodium adduct of GSH**
6.	444.74	**Na_6 – GSH**	**Sodium adduct of GSH**
7.	522.27	**Ag_2SG**	**Glutathione adduct with 2 Ag**
8.	567.80	**(Na-Ag_2GSH)-H_2O**	**Hydrated sodium adduct of Ag_2 cluster**
9.	633.71	**Ag_3 – GSH**	**Ag_3 clusters**
10.	676.08	**Ag_3- SG Na_2**	**Ag $_3$ clusters**
11.	731.48	**[Ag_3- GSH Na_2].(H_2O)$_3$**	**Hydrated form of Ag_3 clusters**
12.	822.71	**(Ag_3 -GSH COONa) (O_2)$_4$**	**Ag_3 Clusters**
13.	844.69	**(Ag_3 SG COONa2) (O_2)$_4$**	**Ag_3 Clusters**
14.	862.70	**(Ag_3 SG COONa2)H_2O (O_2)$_4$**	**Ag_3 Clusters**
15.	876.69	**Ag_5 GSH (BH_4)$_2$**	**Ag_5 clusters**
16.	1033.69	**Ag_5 GSH Na_3 (O_3)HCOONa**	**Ag_5 clusters**
17.	1048.30	**Ag_5 GSH Na_3 (O_5)HCOONa**	**Ag_5 clusters**
18.	1065.64	**Ag_5 GSH Na_3 (O_5)HCOONa**	**Ag_5 clusters**

3.7 Anti-fungal activity of Ag clusters on pathogenic and non-pathogenic fungi by measuring optical density (OD) of the cells using Biophotometer (growth curve assay).

The ability of silver nanoclusters to inhibit fungal growth was checked using different types of Ag nanoclusters in comparison with a control sample (without clusters) on both types of fungal (pathogenic and non pathogenic) using growth curve method, at optical density 600 nm. Pathogenic fungal activity was checked on *Candida albican* fungus and non pathogenic fungal activity was checked on *saccharomyces cerevisiae* fungus as shown in figure 20. In the control experiment where no Ag clusters were added, fungal growth was observed more as compared to the solution in which Ag NCs were present[35]. This happens only in the case of pathogenic fungus. When we did the same experiment with non-pathogenic fungus there is no significance difference between growth curves of control and Ag NCs mixed solution, as shown in figure 22. Anti-fungual activity increases as we increase concentration of Ag clusters as shown in figure 21.

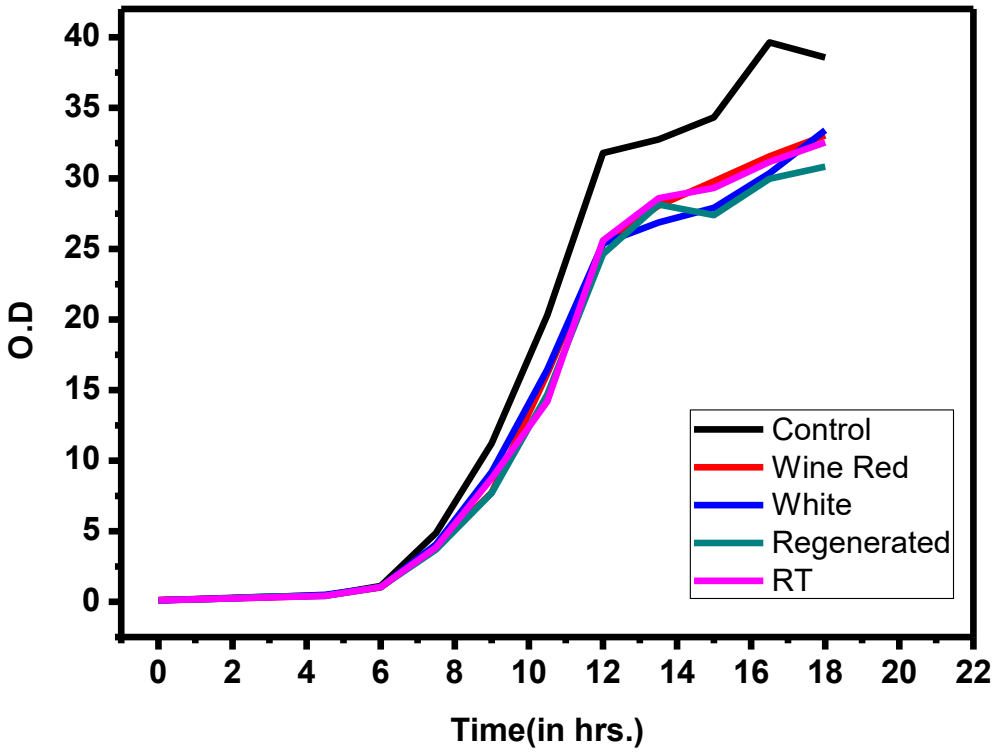

Figure 20. *Growth curve of Candida ablician in the absence of Ag NCs (control) and in the presence of different types of Ag nanoclusters showing difference in the growth curve.*

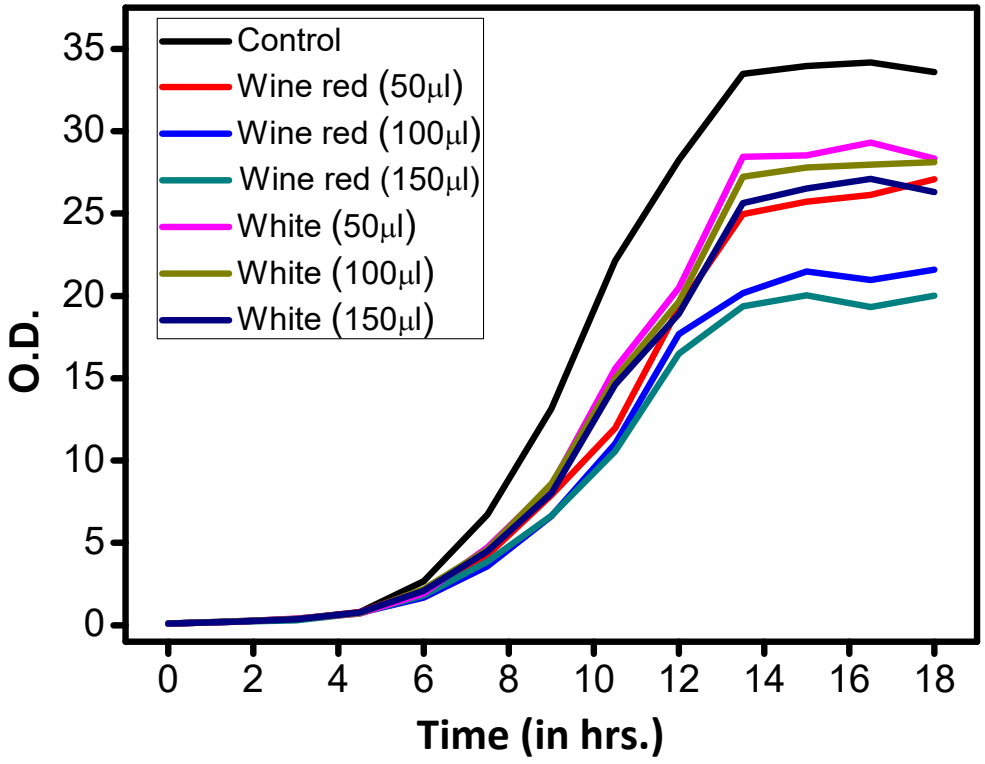

Figure 21. *Anti-fungal activity of Ag clusters with different concentrations.*

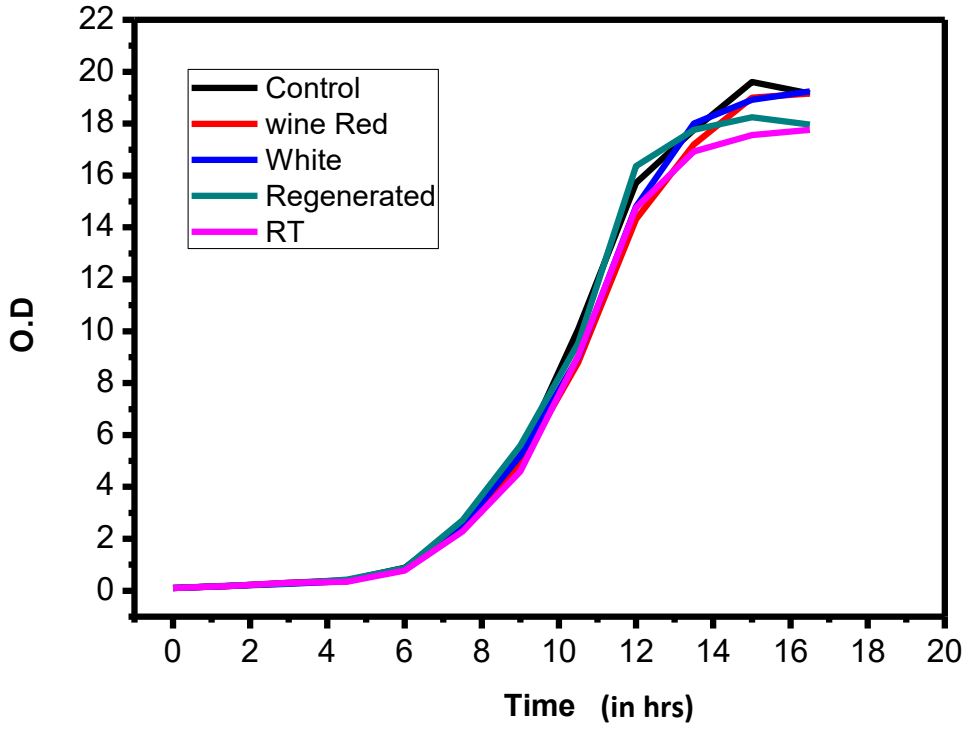

Figure 22. *Growth curve of Saccharomyces cerevisiae in the absence of Ag NCs (control) and in the presence of different types of Ag nanoclusters showing no difference in the growth curve.*

3.8 Growth assay by dilution spotting

Antifungal activity of Ag NCs was also checked by using dilution spotting experiment. The presence of Ag NCs prevents the growth of the *Candida ablician* fungus. In the control plate where no Ag NCs were added, they showed higher density of fungal cells as compared to the plates in which Ag NCs were added. The presence of Ag NCs in the growth media prevented the fungul growth as shown in figures 23(a), (b), (c), (d) taken at different time interval, thus confirming the antifungal activity of nanoclusters.

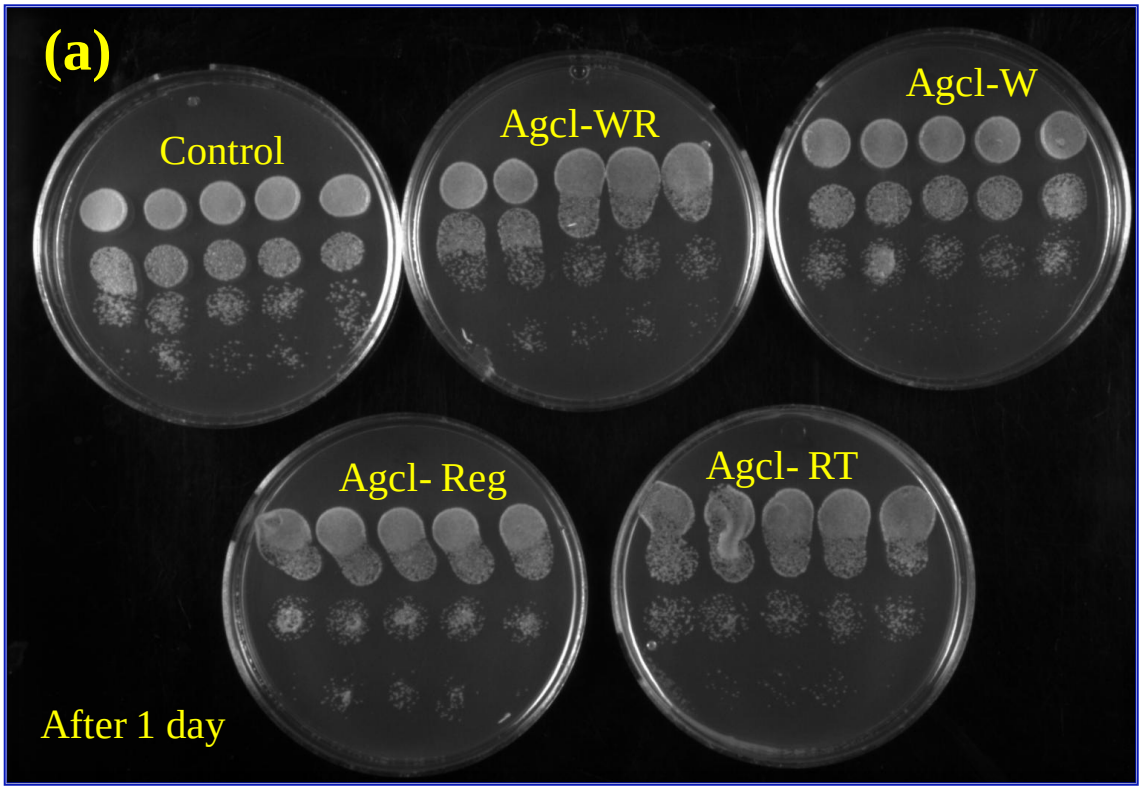

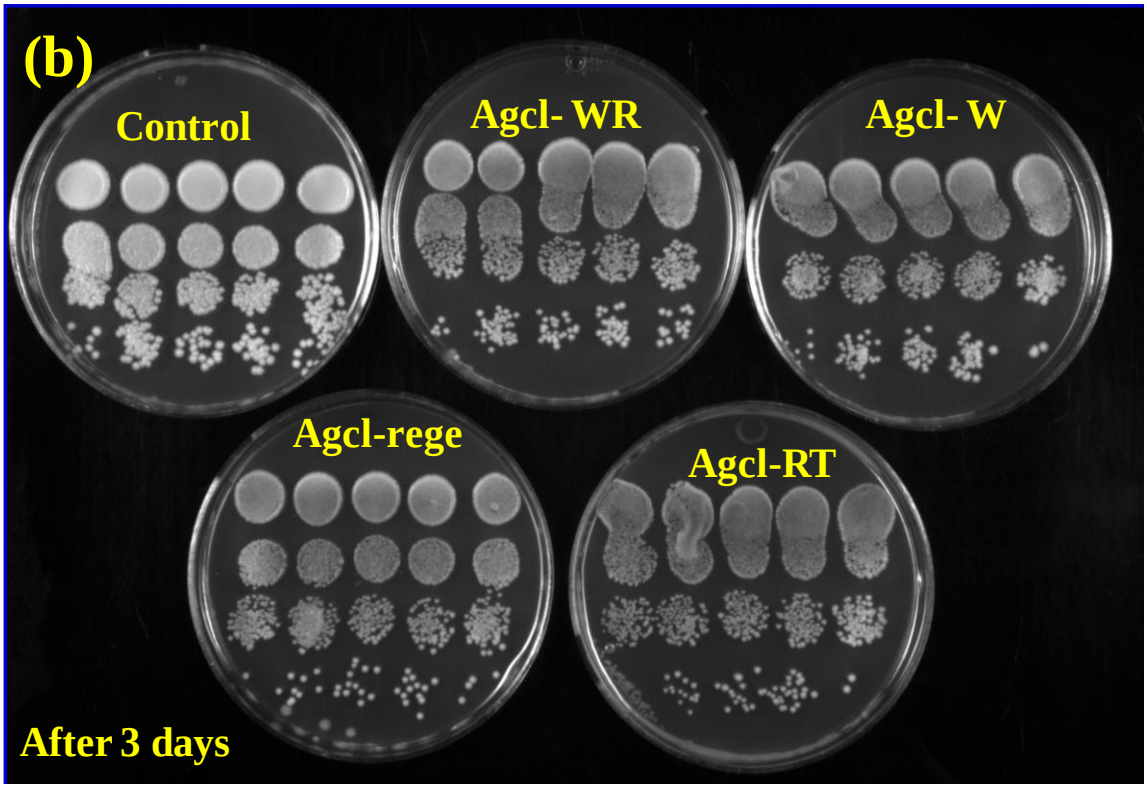
(b)
Control
Agcl- WR
Agcl- W
Agcl-rege
Agcl-RT
After 3 days

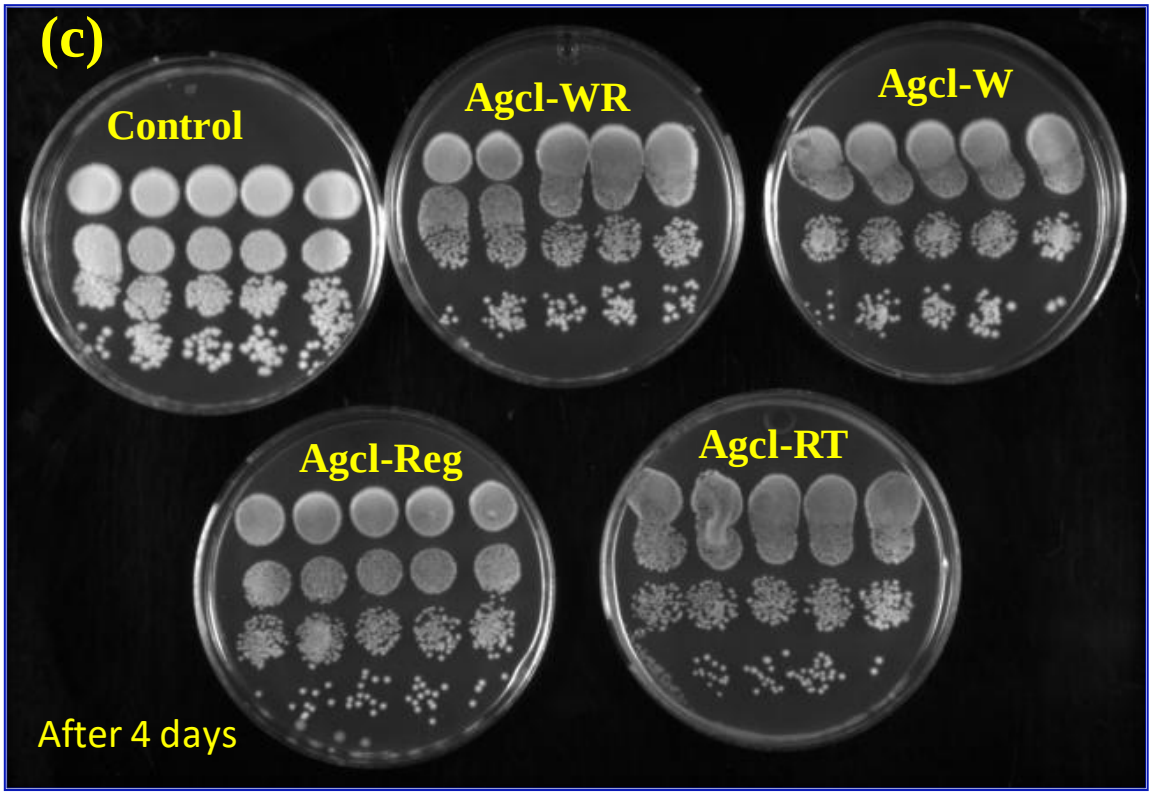
(c)
Control
Agcl-WR
Agcl-W
Agcl-Reg
Agcl-RT
After 4 days

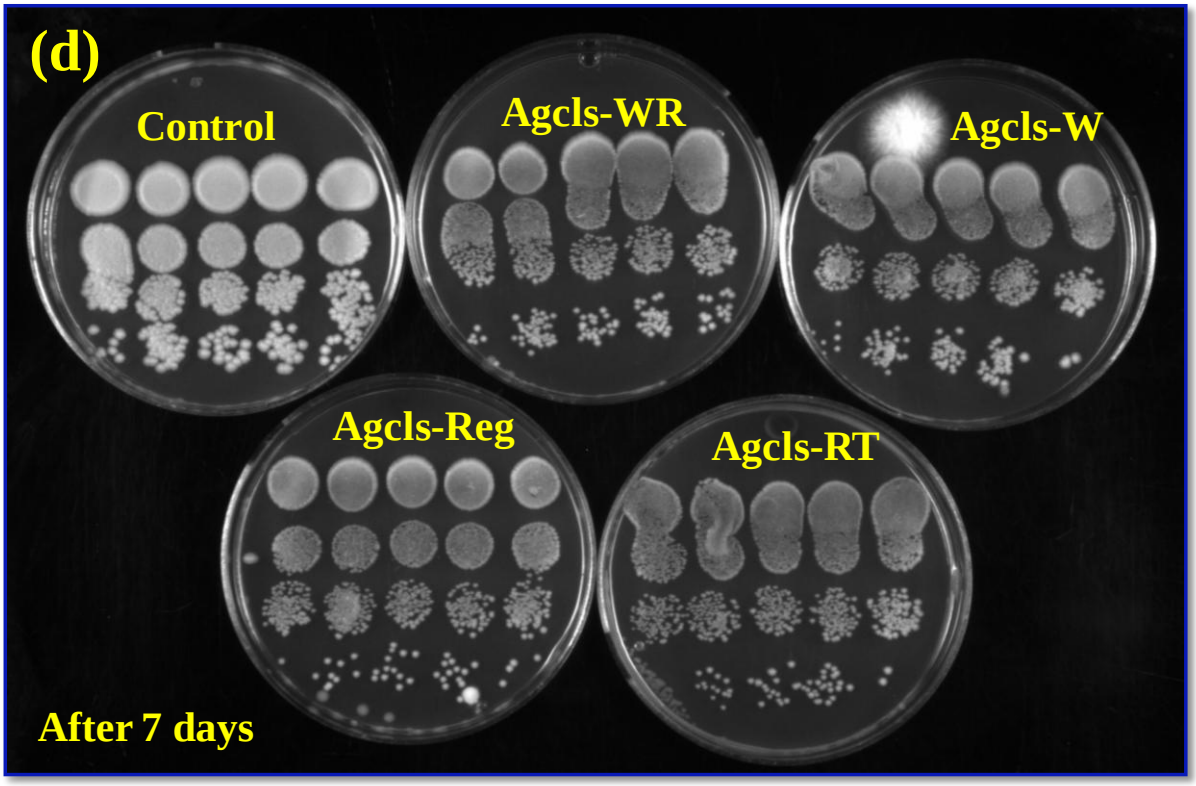

Figure 23. *Cell growth comparison of Candida albcian at different time.*

3.9 Powder X-ray Diffraction (PXRD) study

Figure 24a, b, c and d shows PXRD pattern of wine red, white, regenerated and room temperature Ag clusters respectively. All silver clusters are showing same PXRD pattern, showing peak at 2θ = 38.5˚. This peak is very close to Ag (111) spacing in the bulk and has been attributed to diffraction from silver lattice from glutathione protected Ag clusters[25]. In the case of white Ag clusters, reappearance of peak at around 2θ = 38.5 ˚occurs, but the peak is not as sharp as compare to wine red Ag clusters.

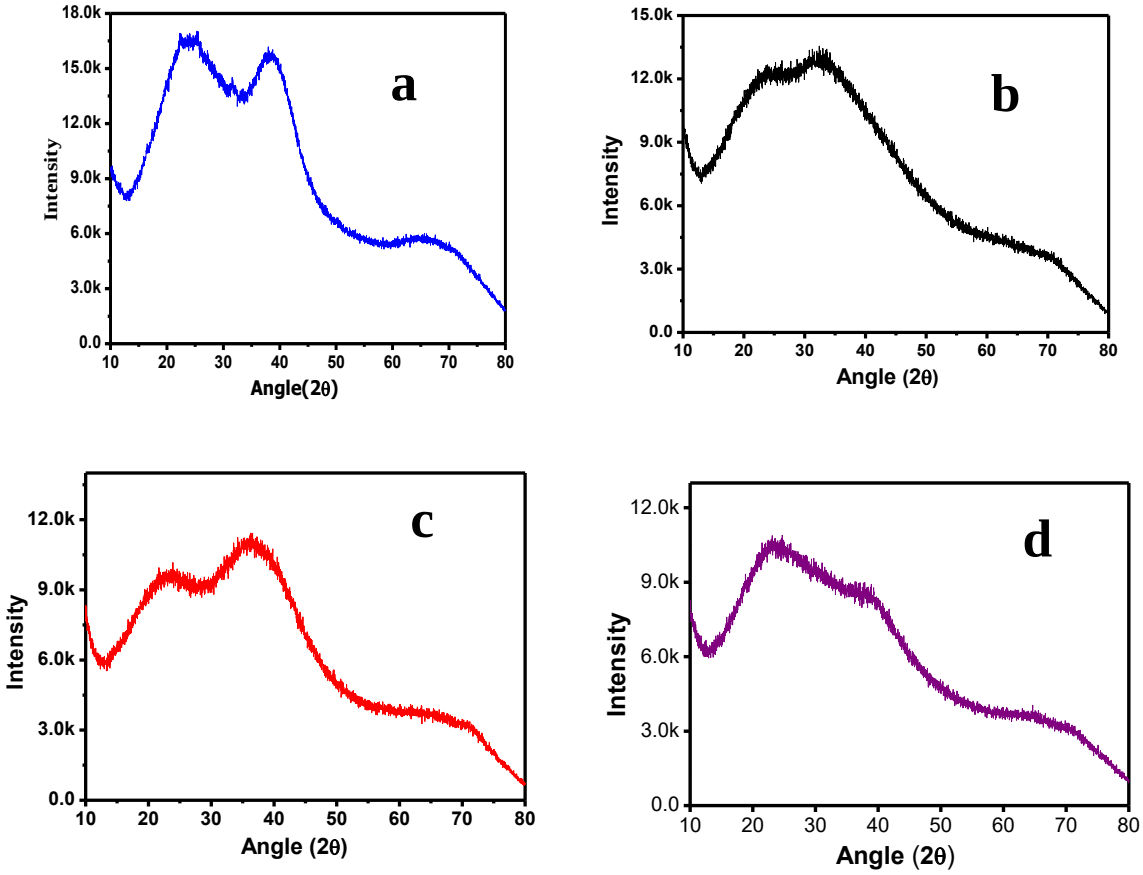

Figure 24. *PXRD pattern of (a). Wine red Ag clusters (b). White Ag clusters (c). Regenerated Ag clusters (d). RT Ag clusters*

The full width half maximum (***FWHM***) of this peak is comparable with the previous Ag cluster report. The broad XRD pattern inferred that the formed Ag in cluster level and not in the form of big nanoparticles or bulk silver lattice.

3.10 Thermogravimetric analysis

In order to monitor Ag content in the glutathione encapsulated Ag clusters we performed Thermogravimetric analysis under inert atmosphere. As shown in figure 25, Ag clusters undergo weight loss from a temperature of 39˚C. At temperature 625 ˚C weight loss is 54%. From this information we can conclude that red wine Ag clusters having 46% Ag and 54 % glutathione. White clusters undergo weight loss from a temperature of 40˚C. At 640 ˚C weight loss is 65%. From this, we can conclude that white clusters having 35% Ag and 65% glutathione.

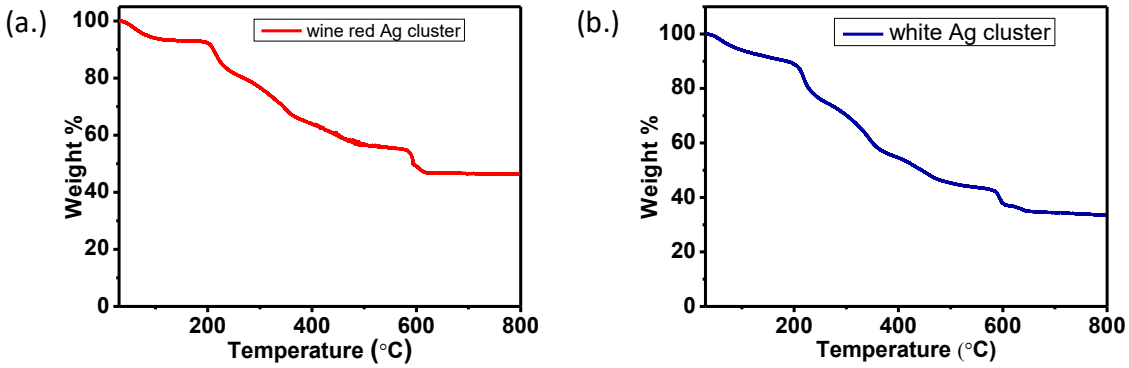

Figure 25. *Thermo-gravimetric profiles of (a) wine red Ag clusters and (b) white Ag clusters.*

4. Conclusion

Anti-microbial activity of glutathione protected Ag clusters was studied and the preferential anti-fungal activity has been observed. As synthesised Ag clusters stability has been studied and analysed. The degraded Ag clusters was not in the form of either silver oxide or silver ions, which was confirmed by control experiment against silver nitrate solution and UV-Vis analysis. We hope, these experimental evidences open new avenue in the field of metal clusters, in particular metal cluster properties. We have analysed thoroughly the anti-fungal activity of freshly prepared Ag clusters and degraded clusters. The degraded clusters are not showing any appreciable changes in fungal activity as compared to wine red Ag clusters. During cluster degradation, the colour changes were discussed through UV-Vis spectroscopy. In this whole thesis of discussion, we found, there is no relation between electronic arrangements with anti-fungal activity.

Every heterogeneous catalyst's catalytic activity depends on the electronic structure of metals nanoparticles, which could be investigated through UV-Vis. We have observed same anti-fungal activity with different electronic structure Ag clusters. Hence, this work is serenely showing difference between heterogeneous catalyst and anti-fungal activity.

1. It may open up new avenues towards the understanding of anti-fungal activity with the help of our hypothesis and the preferential anti-fungal activity with pathogenic-fungus, inferring the selective action of glutathione protected Ag clusters.
2. This selective action and molecular nature of metal clusters may open new way to synthesis a metal nanoparticles derived API (active pharmaceutical ingredients).
3. The further investigations of this work, we are planning to check anti fungal activity and selectivity with different types of capped Ag clusters (capping agent directed anti fungal activity).
4. Antimicrobial activity of Ag clusters will be investigated with different types of transporters, which can support the capping agent mass transport across cell membrane.

With the above conclusions and motivation, here I would like to finish these studies.

Bibliography

1. Xu, H; Suslick, K.S. *Adv mat.*, **2010**, 22, 1078-1082.
2. Tsukuda, Tatsoya; Koyaso, Kiichirou; Yamazoe, Seiji; Takano, Shinjiro. *J.Am. Chem. Soc*., **2015**, 137, 7027-7030.
3. Xie, Jianping; Yuan, Xun; Tay, Yuanqi; Dou, Xinyue; Luo, Zhentao; Leong, David Tai. *Ana. Chem*., **2013**, 85, 1913-1919.
4. Chan, Warren C.W., Nie, Shuming; *Science*, **1998**, 281, 2016-2018.
5. Dickson, Robert M.; Richards, Chris.; Choi, Sungmoo; Hsiang, Jung-Cheng; Antoku, Yasuko; Vosch, Tom; Bongiorno, Angelo; Tzeng, Yih-Ling.. *J. Am. Chem. Soc*, **2008**, 130, 5038-5039.
6. Li, Chang Ming; Xie, jia le; Gio, Chun Xian. *Energy Environ. Sci.*, **2014**, 7, 2559-2579.
7. Chang, Walter H.; Lin, Cheng-An J.; Lee, Chih-Hsien; Hsieh, Jyun-Tai; Wang, Hsueh-Hsiao; Li, Jimmy K.; Shen, Ji-Lin; Chan, Wen- Hsiung; Yeh, Hung-I. *J. Med. Biol. Eng.* **2009**, 29, 276-283.
8. Ying, Y.; Xie, Jianping; Zhenge, Yuangang. *J. Am. Chem. Soc.* **2009**, 131, 888-889.
9. New, S.Y.; Lee, S.T.; Su, X.D. *Nanoscale* , **2016**, 8, 17729- 17746.
10. Xie, Jianping; Luo, Zhentao; Zheng, Kaiyuan. *Chem. Commun*. **2014**, 50, 5143 – 5155.
11. Sun,Di; Liu, Fu-Jing; Huang, Rong-Bin; Zheng, Lan-Sun. *Inorganic Chemistry*, **2011**, 50, 12393-12395.
12. Henon, Norman; Wang, ying; Eckert, Hellmut. *J. Am. Chem. Soc.* **1990**,112, 1322-1326
13. Stevenson, Keith J.; Johnson, Justin A.; Makis, John J.; Marvin, Katherine A.; Rodenbusch, Stacia E. *J. Phys. Chem.C*, **2013**, 117, 22644-22651.
14. K. L. N. Phani; SS, Kumar; C. Jeyabharathi. *Angewchem Int. Edt.* **2010**, 16, 2925-2928
15. Haiss, Wolfgang; Thanh, Nguyen T. K.; Aveyard, Jenny; Ferni, David G. *Anal. Chem*.**2007**, 79, 4215-4221.
16. a. Niska, Karolina; Knap,Narcyz; Kedzia, Anna; Jaskiewicz, Maciej; Kamysz, Wojciech.*International Journal of Medical Science*, **2016**, 13, 772-782.b Laurentius, Lars; Stoyanov, Stanislav; Gusarov, Sergey; Kovalenko, Andriy; Du, Rongbing; lopinski, Gregory P.; McDermott Mark T. *ACS Nano* , **2011**, 5, 4219-4227

17. Y. Negishi, K. Nobusada and T. Tsukuda, *J. Am. Chem. Soc*., **2005**, 127, 5261–5270.
18. S. Kumar; M. D. Bolan; T. P. Bigioni. *J. Am. Chem. Soc*., **2010**, 132, 13141–13143.
19. Y.Yu; Q. Yao; Z. Luo; X. Yuan; J. Y. Lee and J. Xie, *Nanoscale*, **2013**, 5, 4606–4620.
20. Yuan, X.; Luo, Z.; Zhang, Q.; Zhang, X.; Zheng, Y.; Lee, J.Y.; Xie,J. *ACS Nano*, **2011**, 5, 8800–8808.
21. Q. Yao, Y. Yu, X. Yuan, Y. Yu, J. Xie and J. Y. Lee, *Small*, **2013**, 9, 2696–2701.
22. Dong, Jiang Xue; Gao, Zhong Feng; Zhang, Ying; Li, Bang Lin; Li, Nian Bing; Luo, Hong Qun. *Biosensors and Bioelectronics*, **2017**, 91, 155-161.
23. Shukla, Ravi; Bansal, Vipul; Chaudhary, Minakshi; Basu, Atanu; Bhonde, Ramesh R; Sastry, Murali. *Langmuir*, **2005**, 21, 10644-10654
24. Li,Xiaoming; Wang, Lu; Fan, Yubo, Feng, Qingling; Cui, Fu- zhai. *Journal of Nanomaterials*, **2012**, 2012, 19-38.
25. Chen, Chen; Yuan, Zhiqin; Chang, Huan-Tsung; Lu, Fengniu; Li, Zenghe; Lu, Chao. *Anal. Method*, **2016**,8, 2628-2633.
26. Fujigaya, Tsuyohiko; Kim, Chae, Rin; Hamasaki, Yuki, Nakashimal, Naotoshi, *Nature Scientific Reports*, **2016**, 2134-21324.
27. Teka, Libor Kvi; Panacek, Ales; Kolar, Milan; Vecerova, Renata; Prucek, Robert; Soukupova, Jana; Krystof, Vladimir; Hamal, Petr; Zboril, Radek; Kvitek, Libor.*Biomaterials*, **2009**, 30, 6333-6340.
28. Bharadwaj, Niranjan Dev; Sharma, Arvind Kumar. *IJRASET*, **2016**, 4, 2321-9653.
29. Martins, Natalia; Ferreira, Isabel; Barros, Lillian; Silva, Sonia; Henriques, Mariana. *Mycopathologia*, **2014**, 177, 223-240.
30. Javani, Siamak; lorca, Romina; latorre, Alfonso; Flors, Cristina; Cortajarena, Aitziber L. *Appl. Mater. Interfaces*, **2016**, 8, 10147-10154.
31. Hyllested, Jes; Palanco, Marta Espina; Hagen, Nicolai; Mogensen, Klaus Bo; Kneipp, Katrin. *Beilstein J. Nanotechnol*. **2015**, 6, 293-299.
32. Brousseau, Louis ; Novak, James p. ; Marinakos, Stella M.; Feldhelm, Daniel L. *Adv. Mater.*, **1999**, 11, 6.
33. Kumar, Santosh; Bolan, Michael D.; Bigioni, Terry P. *J.Am. Chem. Soc.*, **2010**, 132, 13141-13143.

34. Krsti, marjan; Zavras, Athanasios; Khairallah, George N.; Dugourd, Philippe; Koutecky Bona, Vlasta; O'Hair, Richard A. J. *International. Journal of mass Spectroscopy*, **2017**, 413, 97-105.
35. Schacht, V.J.; Neumann, L.V; Sandhi, S.K.; Chen, L.; Henning,T; Klar, P.J; Theophel, K.; Schell, S.; Bunge, M. *Journal of Appl. Microbio*, **2012**, 114, 25-35.